Optical variability of seawater in relation to particle concentration, composition, and size distribution in the nearshore marine environment at Imperial Beach, California

Sławomir B. Woźniak,[1,2] Dariusz Stramski,[2] Malgorzata Stramska,[3] Rick A. Reynolds,[2] Vanessa M. Wright,[2] Ezra Y. Miksic,[2] Marta Cichocka,[2] and Agnieszka M. Cieplak[2]

Received 5 June 2009; revised 19 March 2010; accepted 5 April 2010; published 25 August 2010.

[1] We examined optical variability of seawater in relation to particle concentration, composition, and size distribution in the nearshore marine environment at Imperial Beach, California, over a period of 1.5 years. Measurements included the hyperspectral inherent optical properties (IOPs) of seawater (particulate beam attenuation, particulate and CDOM absorption coefficients within the spectral range 300–850 nm), particle size distribution (PSD) within the diameter range 2–60 μm, and the mass concentrations of suspended particulate matter (SPM), particulate organic carbon (POC), and chlorophyll *a* (Chl). The particulate assemblage spanned a wide range of concentrations and composition, from the dominance of mineral particles (POC/SPM < 0.06) with relatively steep PSDs to the high significance or dominance of organic particles (POC/SPM > 0.25) with considerably greater contribution of larger-sized particles. Large variability in the particulate characteristics produced correspondingly large variability in the IOPs; up to 100-fold variation in particulate absorption and scattering coefficients and several-fold variation in the SPM-specific and POC-specific coefficients. Analysis of these data demonstrates that knowledge of general characteristics about the particulate composition and size distribution leads to improved interpretations of the observed optical variability. We illustrate a multistep empirical approach for estimating proxies of particle concentration (SPM and POC), composition (POC/SPM), and size distribution (median diameter) from the measured IOPs in a complex coastal environment. The initial step provides information about a proxy for particle composition; other particulate characteristics are subsequently derived from relationships specific to different categories of particulate composition.

Citation: Woźniak, S. B., D. Stramski, M. Stramska, R. A. Reynolds, V. M. Wright, E. Y. Miksic, M. Cichocka, and A. M. Cieplak (2010), Optical variability of seawater in relation to particle concentration, composition, and size distribution in the nearshore marine environment at Imperial Beach, California, *J. Geophys. Res.*, *115*, C08027, doi:10.1029/2009JC005554.

1. Introduction

[2] Knowledge and understanding of optical variability in seawater is important for many scientific and practical problems in ocean sciences, and is particularly relevant in optically complex coastal and nearshore environments. Because of highly dynamic oceanographic processes as well as terrestrial and anthropogenic effects in these environments, the optically significant particulate and dissolved constituents of water typically undergo large variations, which are accompanied by correspondingly large variations in the optical properties. In recent years, the development of new sensors and diverse in situ, airborne, and spaceborne platforms has enabled observations over a wide range of temporal and spatial scales. A number of special research programs have been devoted to the study of coastal ocean with a major support provided by optical measurements, including relatively high resolution time series measurements [e.g., *Dickey and Chang*, 2001; *Dickey*, 2004]. In these programs, the optical signatures and measurements have been shown to provide highly complementary and powerful means for studying various physical and biogeochemical processes as well as for bottom characterization in sufficiently shallow environments [e.g., *Chang et al.*, 2002; *Coble et al.*, 2004; *Philpot et al.*, 2004; *Weisberg et al.*, 2004; *Schofield et al.*, 2006].

[3] While instrumentation and platforms to measure optical properties have undergone rapid advancement, there

[1]Institute of Oceanology, Polish Academy of Sciences, Sopot, Poland.
[2]Marine Physical Laboratory, Scripps Institution of Oceanography, University of California, San Diego, La Jolla, California, USA.
[3]Center for Hydro-Optics and Remote Sensing, San Diego State University, San Diego, California, USA.

0148-0227/10/2009JC005554

remains a need for better interpretations of present optical measurements in terms of water constituents because they are directly responsible for the observed optical variability. In addition to variations in particle concentration, the major sources of variability in particulate optical properties include the particle size distribution and composition, the latter being a determinant of the particle refractive index [*Bohren and Huffman*, 1983; *Jonasz and Fournier*, 2007]. The optically significant particle sizes in aquatic environments cover a wide range from submicrometer sizes to tens or hundreds of micrometers, and the particle size distribution can exhibit significant variations in time and space [e.g., *Jonasz and Fournier*, 2007]. Similarly, the refractive index of aquatic particles can vary considerably. Mineral particles generally have much higher values compared with organic particles, which often contain a significant amount of intracellular water and thus exhibit fairly low values for the refractive index relative to surrounding water [e.g., *Aas*, 1996; *Kerr*, 1977]. Historically, however, these key characteristics of particulate assemblages have been greatly undersampled in field optical experiments, largely because the measurements of these particle characteristics are often not fully amenable to in situ methods. Analytical techniques as applied to discrete water samples are required, but unfortunately have been often too limited or beyond the design capacity of field programs involving in situ optical measurements. Further advances in our understanding of optical observations require a concerted effort of simultaneous measurement of a comprehensive set of optical properties and the characterization of optically significant constituents in terms of both their concentrations and composition, including the particle size distribution.

[4] In line with these needs, there has been a recent considerable increase in research efforts focused on relations between the water inherent optical properties (IOPs) and water constituents in coastal regions. For example, *Babin et al.* [2003b] reported on variations in light absorption coefficients of phytoplankton, nonalgal particles, and color dissolved organic matter (CDOM) in relation to mass concentration of suspended particulate matter (SPM) and concentration of phytoplankton pigments in different coastal waters around Europe. Another work based on the same experiments addressed the relationships between the scattering coefficient of marine particles and SPM concentration [*Babin et al.*, 2003a]. Other examples of coastal and nearshore environments that were investigated in terms of linkages between the variability of IOPs and water constituent concentrations and/or composition include the New England shelf [*Green et al.*, 2003], a shallow embayment within the Chesapeake Bay [*Gallegos et al.*, 2005], shelf waters in the Irish Sea [*McKee and Cunningham*, 2006], tropical coastal waters of eastern Australia [*Oubelkheir et al.*, 2006], eastern English Channel [*Vantrepotte et al.*, 2007], and coastal waters off New Jersey, the Northern Gulf of Mexico, and Monterey Bay [*Snyder et al.*, 2008; *Stavn and Richter*, 2008]. Not surprisingly, as the key particle characteristics affecting optics can vary significantly in aquatic environments, previous studies show a wide range of particulate IOPs, even upon the normalization to measurable proxies of bulk concentration of the entire (or nearly entire) particulate assemblage such as SPM, or bulk concentrations representing certain components of particulate assemblage, such as chlorophyll *a*, POC (particulate organic carbon), POM (particulate organic matter), or PIM (particulate inorganic matter).

[5] This variability poses challenges for both in-depth interpretation of optical data and the development of robust inverse algorithms for estimating biogeochemically important water constituents with consistently good accuracy. Ideally, these challenges would be best addressed if measurements could provide a complete characterization of both the high spectral resolution IOPs from the ultraviolet (UV) to near infrared (NIR) and all optically significant characteristics of water constituents, including the concentrations of various particle types which have different sizes, refractive indices, and morphologies [*Stramski et al.*, 2001]. Practically, such an idealized experimental design is not achievable, especially in field studies. However, further incremental progress to improve understanding of IOPs in relation to water constituents is certainly possible through enhancements of measurement capabilities and experimental designs. To our knowledge, for example, none of the previous field studies includes the simultaneous measurements of hyperspectral absorption and scattering coefficients from the UV to NIR, particle size distribution (PSD), and particulate composition. Because both the size and composition are the key determinants of particle optical properties, a need for routine determinations of these particle characteristics as part of optical experiments is particularly important.

[6] In this study we report on experimental data collected in nearshore waters at Imperial Beach located within San Diego County in Southern California. A key feature of this study was collection of a comprehensive set of optical data that include hyperspectral absorption and scattering coefficients from the UV to NIR in conjunction with characterization of particulate concentration, size distribution, and a proxy of composition expressed as the contribution of particulate organic carbon (POC) to the particulate mass concentration (SPM). Measurements and analysis of discrete water samples were conducted using laboratory techniques and instrumentation. To cover a wide range of environmental situations, water sampling and subsequent measurements were made systematically every 2 weeks, or occasionally more often, for a period of about 1.5 years.

[7] The primary objective of this study is to examine optical variability in the complex nearshore environment in terms of key characteristics of suspended particulate matter. Using observations derived from this data set, we illustrate an approach for building empirical algorithms with potential for improved estimation of particle characteristics from measured IOPs in optically complex aquatic environments. This approach is based on a suite of empirical relationships that utilize collective information characterizing the IOPs and the particle assemblage, i.e., metrics describing particle concentration, composition, and size distribution. The conceptual basis of the approach is that the relationships between the IOPs and the metrics of particle concentration and size are established separately for distinct subsets of data which represent different particulate composition. This feature of the approach is expected to reduce the large natural variability normally seen in common empirical algorithms which parameterize optical properties in terms of a single measure of particle concentration and are applied to data sets that

may encompass a wide range of particulate composition. We use the ratio of POC/SPM (i.e., the ratio of the concentration of particulate organic carbon, POC, to the mass concentration of suspended particulate matter, SPM) as an indicator for particulate composition and partitioning of our data into the composition-related particle groups. Alternative metrics for particulate composition could be used as well, and the choice of POC/SPM in this study has no particular significance to the general concept of our approach. We also note that although our approach is demonstrated with data from one region, the conceptual basis is applicable to any environment, and could prove to be particularly fruitful in optically complex waters such as those found in marine coastal environments.

2. Methods

2.1. Water Sampling

[8] The nearshore location for collecting seawater samples was at a pier in the City of Imperial Beach, San Diego County, California (latitude of 32°35′N and longitude 117°8′W). Imperial Beach is located within the Tijuana River watershed and the Imperial Beach Pier (IBP) is ~2.8 km north of the Tijuana River mouth and approximately 5 km north of the US-Mexican border. We made experiments on 44 days between December 2004 and July 2006 at the IBP. The experiments consisted of laboratory measurements and analysis of the collected water samples. Samples of the surface water were collected with a bucket from the end of the pier about 400 m from the shoreline, where the average bottom depth is about 10 m. Collected samples were stored in clean containers (Nalgene), and immediately transported to our laboratory at the Scripps Institution of Oceanography for further analysis.

[9] Sampling was made about every 2 weeks and occasionally more often during a period of rainstorm events in winter 2005. The overall length of the study spanning about 1.5 years enabled us to sample under different environmental situations throughout different seasons. As a result, we covered a wide range of optical variability caused by various phenomena, including the most prominent effects associated with episodic rainstorm events (Tijuana River discharge, stormwater runoff, and bottom resuspension) and massive phytoplankton blooms (red tides).

2.2. Concentrations of Seawater Constituents

[10] The concentration of suspended particulate matter, SPM [units are g m^{-3}], defined as the dry mass of particles per unit volume of water, was determined using a standard gravimetric technique. We used preweighed glass-fiber GF/F filters (25 mm in diameter) for filtration of measured volumes of seawater samples (between 50 and 500 mL). At the end of filtration, sample filters were rinsed with deionized water to remove sea salt. The dry mass of particles collected on the filters was measured with a Mettler-Toledo MT5 microbalance (resolution 0.001 mg). The particle mass retained on the filter was, on average, 1.86 mg (standard deviation SD = 0.66 mg). Three replicate filters were measured in each experiment, with the reproducibility generally within ±17%.

[11] We estimated that our SPM determinations are potentially subject to a mean error of +10% (SD = 3%). The minimum and maximum estimated errors based on consideration of the individual samples are 4% and 22%, respectively. These values were calculated from estimates concerning two types of error, which act in opposite direction and therefore reduce the final bias. The first type of error is related to the loss of filter mass during the filtration process, and leads to an underestimation of SPM. This error could, in principle, be avoided by making the analysis on filters prewashed with an appropriate quantity of pure deionized water. The second type of error, leading to an overestimation of SPM, is associated with incomplete removal of sea salt during rinsing with deionized water after sample filtration [*Trees*, 1978; *Stavn et al.*, 2009].

[12] On the basis of special experiments in which the filter mass loss was determined as a function of volume filtered, we estimated that the first error was on average −6% (SD = 2%). The water salinity at the location of our study site varies within a very restricted range throughout the year, being on average 33.48 psu and dropping sporadically only slightly to about 33 psu after heavy rainstorm events (E. Terrill, personal communication, 2009). Using the results of the study by *Stavn et al.* [2009] for water salinity of 33 psu and after appropriate conversion to represent the use of 25 mm filters, we estimated that the salt retention error could be, on average, +18% (SD = 7%). That study suggests that the maximum mass of salt retained on the 25 mm filter for salinity of 33 psu is about 0.25 mg, which is significantly less than the particle mass retained on the filters in our experiments. The above estimations suggest that the errors associated with the filter mass loss and salt retention probably did not completely compensate for one another in our experiments, resulting in a possible average error of about +10%. We did not apply a correction for this error because of the uncertainty in the estimation of salt retention error and relatively high variation between our replicate SPM determinations (±17%). To achieve a correction for salt retention with sufficiently high level of confidence would require additional determinations of the so-called "absolute procedural control" specific to a given measurement protocol and conditions of particular experiment (e.g., filter size, volumes filtered, particle load on filters, water salinity), as recommended by *Stavn et al.* [2009]. Whereas this is a desirable improvement of the SPM methodology, it is not yet commonly made and has not been performed in our experiments.

[13] Particles were also collected by filtration on precombusted GF/F filters (three replicates per each experiment) for the analysis of particulate organic carbon (POC) concentration and particulate organic nitrogen (PON) concentration [g m^{-3}]. The sample filters were dried after filtration and stored until analysis with a high temperature combustion technique. The reproducibility of replicate measurements of POC was generally within ±8%. Additional samples were taken for the analysis of phytoplankton pigment concentrations. Particles collected on GF/F filters were stored in liquid nitrogen and analyzed at a later time with HPLC and fluorometric techniques. Data in this paper utilize the concentrations of chlorophyll *a*, Chl, obtained with the fluorometric method [*Trees et al.*, 2002].

[14] We use the POC/SPM ratio for partitioning our data set into three groups characterizing particulate composition, which we refer to as mineral-dominated, organic-dominated,

and mixed (more details in section 3.2). In general, samples with very low POC/SPM ratio are expected to have a dominant mass contribution of mineral particles as compared with organic particles. An increase in POC/SPM will generally indicate an increase in the contribution of organic particles. Although there is no unique conversion of POC to the total mass concentration of particulate organic matter, the use of POC is valuable because of potential applications of optical measurements to questions related to carbon biogeochemistry. Because plankton is an important component of particulate organic matter, the significance of POC within the context of optical approaches also stems from the fact that the intracellular content of carbon is linked to the optically significant properties of plankton cells, their size and refractive index [*Montagnes et al.*, 1994; *Stramski*, 1999; *Menden-Deuer and Lessard*, 2000; *DuRand et al.*, 2002].

[15] An alternative characterization of particulate composition could be achieved with the loss on ignition (LOI) technique, which partitions SPM into the mass concentrations of particulate organic matter (POM) and particulate inorganic matter (PIM) [*Pearlman et al.*, 1995; *Barillé-Boyer et al.*, 2003; *Stavn et al.*, 2009]. While the LOI technique would provide useful complementary information for our data analysis, we did not use this technique because of logistical constraints in our experiments. It must also be emphasized that the parameters POC, POM, and PIM all represent simple proxies for particulate composition as defined at a fairly rudimentary level. In reality, variable composition of natural particulate assemblages and their implications to optics are certainly more complex than described by just two types of particles, organic and inorganic (or POC and non-POC types).

2.3. Particle Size Distribution

[16] The particle size distribution (PSD) was measured with a Coulter Multisizer III (Beckman-Coulter) using an aperture tube with a diameter of 100 μm, which allows coverage of the particle size range between 2 μm and 60 μm with very high resolution. Each PSD measurement provided a set of values representing the number of particles per unit volume of sample, $N(D)$ [units used in this paper are cm^{-3}], within each size bin for 256 logarithmically spaced bins along the axis of equivalent spherical particle diameter, D [μm]. For each sample and the corresponding particle-free reference seawater (i.e., seawater filtered at least twice through a 0.2 μm Nalgene syringe filter), we made at least 3 replicate measurements, each on the volume of 2 mL. The replicates of sample measurement were compared, corrected for the particle-free baseline, and averaged to obtain the final PSD. If necessary, the seawater samples were diluted with filtered seawater prior to measurement to avoid the coincidence effects. The dilution factor was then taken into account in the calculation of the final PSD. Based on the values of $N(D)$, we calculated the density functions of particle number concentration, $F_N(D)$ [cm^{-3} μm^{-1}], and the particle volume concentration, $F_V(D)$ [μm^{-1}]. From the $F_V(D)$ function, we also calculated the total volume concentration of particles within the 2–60 μm range, $C_V^{2-60\mu m}$ [dimensionless], and the two size parameters, D_{V50} and D_{V90} [μm], which respectively represent the median diameter (50th percentile) and the 90th percentile diameter of particle volume distribution. We also tested the median and percentile parameters obtained from particle number and particle projected-area distributions, but found no particular advantage of using these parameters compared with those based on particle volume distribution for the purposes of our study.

[17] We recognize that measurements of the size distribution truncated within the 2–60 μm range represent some limitation as particles outside this range also provide a contribution to the optical properties and particle mass concentration [e.g., *Stramski and Kiefer*, 1991; *Carder and Costello*, 1994; *Jackson et al.*, 1997; *Peng et al.*, 2007]. Practical considerations associated with a broad suite of measurements that required simultaneous execution were the main reason for this limitation in our experiments, but we note that it is desirable and generally possible to extend the size range by using multiple aperture tubes with a Coulter technique and/or multiple techniques for particle sizing.

2.4. Inherent Optical Properties of Seawater

[18] The optical measurements of the beam attenuation and absorption coefficients were made with a double-beam bench-top spectrophotometer (Perkin-Elmer Lambda 18) equipped with a 15 cm integrating sphere (Labsphere RSA-PE-18). The measurements were performed in the spectral range from λ = 300 to 850 nm with a 1 nm interval (where λ is light wavelength in vacuo). As a general rule, our baseline and sample scans were taken in succession with a reference and sample placed in the sample beam during the respective scans. Both baseline and sample measurements were thus made relative to a stable light intensity of reference beam traveling through air. For all optical measurements, a minimum of two replicate spectra were obtained and subsequently averaged.

[19] The spectra of the beam attenuation coefficient of suspended particles, $c_p(\lambda)$ [m^{-1}], were measured using a geometry in which the acceptance angle of the detector was reduced to less than about 0.7° [*Stramski et al.*, 2004b, 2007]. The measurements were made on particles in suspension contained in a 1 cm cuvette. The optical density (referred also to as absorbance in classical spectrophotometry) of particles, $OD_p(\lambda)$, was determined as a difference between the optical density of the sample (i.e., the particle suspension) and the particle-free reference (i.e., seawater prefiltered with GF/F filter and then filtered twice through a 0.2 μm Nuclepore filter).

[20] The values of $c_p(\lambda)$ were calculated by multiplying $OD_p(\lambda)$ by ln(10) and dividing by the pathlength of 0.01 m. Because the measurements were made over a short pathlength on natural water samples, the $OD_p(\lambda)$ signal was generally small (< 0.13 in the visible spectral range) and often showed significant random noise of the instrument. Therefore, the final $c_p(\lambda)$ spectra were obtained by smoothing with a 5-point moving average, which was repeated five times. Although the overall spectral trend and magnitude of the final $c_p(\lambda)$ are reasonably robust, these spectra for most experiments still show small-scale irregularities related to instrument noise. For two experiments with the values of $c_p(\lambda)$ below 1 m^{-1}, the data are not considered due to very low signal. We also note that the optical measurements were made on samples which satisfied the criteria of single scattering regime. Therefore, if necessary (i.e., in the case of very turbid samples), the samples were diluted with particle-free water prior to measurements.

[21] Particulate absorption spectra, $a_p(\lambda)$ [m^{-1}], were also measured with a Perkin-Elmer Lambda 18 spectrophotometer equipped with an integrating sphere. The Transmission-Reflectance (T-R) filter-pad technique was used [*Tassan and Ferrari*, 1995, 2002]. For a given sample, this technique requires the measurement of optical density spectra with at least four different filter-detector configurations involving sample and blank GF/F filters. From these measured optical densities, we calculated the desired value representing the optical density of particles collected on the filter, $OD_s(\lambda)$, following the equations of *Tassan and Ferrari* [1995, 2002]. In these calculations we assumed that the transmittance of the sample filter is identical regardless of whether or not the side of the filter with particles faces the beam. This is a good assumption which allows simplifying the procedure by avoiding an additional transmittance measurement with the particles on the filter facing the entrance to the integrating sphere rather than the incident beam [*Tassan and Ferrari*, 2002].

[22] The correction for the pathlength amplification factor (the so-called β-factor) was applied, in which the optical density of particles on the filter, $OD_s(\lambda)$, was converted to the equivalent optical density of particles in suspension, $OD_{sus}(\lambda)$ [e.g., *Mitchell*, 1990]. We used the formula $OD_{sus}(\lambda) = 0.592\ [OD_s(\lambda)]^2 + 0.4\ OD_s(\lambda)$, which was established with our Perkin-Elmer spectrophotometer based on experiments with several phytoplankton cultures, mineral-rich particulate assemblages, and natural assemblages of particles from marine environments [*Stramska et al.*, 2006]. Finally, the particulate absorption coefficient, $a_p(\lambda)$, was determined by multiplying $OD_{sus}(\lambda)$ by ln(10) and the clearance area of the filter, and dividing this product by the volume of sample filtered. For a few samples with high enough turbidity, we also measured $a_p(\lambda)$ on particle suspension in a 1 cm cuvette placed inside the integrating sphere, thus minimizing the scattering error to a negligible level and obtaining accurate estimates of particulate absorption [see, e.g., *Stramski et al.*, 2007]. The results agreed well with those obtained from the T-R technique, which lends confidence to our T-R determinations.

[23] In order to partition $a_p(\lambda)$ into phytoplankton $a_{ph}(\lambda)$ and nonphytoplankton $a_d(\lambda)$ (commonly referred to as detritus) components, the sample GF/F filters were subject to similar transmittance and reflectance measurements following treatment with sodium hypochlorite NaClO [*Ferrari and Tassan*, 1999]. In this treatment, the particles on the sample filter were exposed to a small amount of a 2% NaClO solution for several minutes with a primary purpose of bleaching phytoplankton pigments. The T-R measurements on the bleached sample filters yielded the estimates of $a_d(\lambda)$. The phytoplankton absorption coefficient, $a_{ph}(\lambda)$, was then obtained as a difference between $a_p(\lambda)$ and $a_d(\lambda)$.

[24] We found that the bleaching technique failed to provide reasonable results for samples with a relatively small contribution of phytoplankton to the overall particulate assemblage. Samples with a very low ratio of Chl to SPM (generally less than 10^{-4}) showed that the derived spectra of $a_{ph}(\lambda)$ were nearly featureless with no characteristic maxima of phytoplankton absorption around 440 nm and 675 nm. This indicated the failure of the partitioning method based on the NaClO bleaching. In contrast, the derived spectra of $a_{ph}(\lambda)$ for samples with higher Chl/SPM clearly showed the presence of the expected spectral features of phytoplankton absorption. For that reason, we will report on the absorption partitioning only for a selected group of samples dominated by organic particles, for which the bleaching method yielded a reasonable shape of the $a_{ph}(\lambda)$ spectra.

[25] We also measured the absorption coefficient of colored dissolved organic matter, $a_{CDOM}(\lambda)$ [m^{-1}], using a Perkin-Elmer spectrophotometer. These measurements were made on samples filtered through a prerinsed 0.2 μm Nuclepore filter relative to freshly made pure water (deionized and particle-free) following the NASA-recommended protocol [*Mitchell et al.*, 2003]. The CDOM sample or pure water reference was put in a 10 cm cylindrical cuvette and measured with a geometrical setup similar to that used for $c_p(\lambda)$. The values of $a_{CDOM}(\lambda)$ were calculated by multiplying the baseline-corrected optical densities $OD_{CDOM}(\lambda)$ by ln(10) and dividing by the pathlength of 0.1 m. Assuming that $a_{CDOM}(\lambda)$ is negligible at wavelengths roughly above 600 nm, any measured offset (typically determined over a 10 nm range between 590–640 nm) was subtracted to obtain the final $a_{CDOM}(\lambda)$. The spectra of the scattering coefficient of particles, $b_p(\lambda)$, were determined as a difference between $c_p(\lambda)$ and $a_p(\lambda)$.

3. Results and Discussion

3.1. General Variability of Constituents and Seawater Optical Properties

[26] During the 1.5 year period of sampling, large changes in the concentration, composition, and size distribution of suspended particulate matter were observed at the study location in Imperial Beach (Table 1). This variability was associated with seasonal patterns in the physical environment (e.g., solar irradiance, rainfall, winds), and also with episodic events on shorter time scales such as winter storms or plankton blooms. Here we do not discuss in detail temporal patterns in the measured variables, but merely state that the resulting database encompasses a diverse range of particle assemblages with varying biogeochemical properties, including suspensions dominated by minerogenic particles, algal cells including red tide events, and various mixtures of inorganic and organic particles.

[27] The greatest variation was observed among measurements pertaining to the particle concentration, i.e., SPM, $C_v^{2-60\mu m}$, POC, and Chl. The variation of SPM was about 34-fold, but $C_v^{2-60\mu m}$, POC, and Chl varied distinctively more than 100-fold (190-fold, 155-fold and nearly 200-fold, respectively; see Table 1). The composition of particulate matter was also highly variable during the IBP experiment as indicated by 18-fold variation in the ratio of POC to SPM (Table 1). A similar range (16-fold) was observed in the POC/Chl ratio.

[28] The variation of two statistical parameters, D_{V50} and D_{V90}, derived from the measurements of particle volume distributions was also examined to characterize changes in the particle size distribution (PSD). The median particle diameter, D_{V50}, divides the size distribution of particle volume into two equal portions within the measured diameter range 2–60 μm. The higher the D_{V50}, the larger the contribution of relatively large particles to the total particle volume. During the course of our experiment, D_{V50} varied significantly between about 4 and 39 μm, which is indicative of large variability in the shape of PSD. Smaller values

Table 1. Range of Variability in the Characteristics of Suspended Particulate Matter and Inherent Optical Properties in the Nearshore Waters at the Imperial Beach Pier

Parameters	Minimum Values for All IBP Samples[a]	Maximum Values for All IBP Samples[a]	Annual Average Values for the IBP Samples for 2005[b]
SPM (g m^{-3})	2.4 (December 2005)	82.3 (July 2005)	13.5 (17.8)
POC (g m^{-3})	0.22 (February 2005)	34.4 (July 2005)	2.33 (6.06)
Chl (mg m^{-3})	1.28 (December 2004)	247.6 (July 2005)	14.9 (43.2)
POC/SPM (g:g)	0.023 (February 2005)	0.42 (July 2005)	0.16 (0.12)
POC/Chl (g:g)	68 (April 2005)	1104 (January 2005)	200 (186)
$C_v^{2-60\mu m}$	9.82×10^{-7} (December 2005)	1.9×10^{-4} (July 2005)	1.2×10^{-5} (3.3×10^{-5})
D_{V50} (μm)	3.7 (February 2005)	39.0 (September 2005)	15.9 (12.4)
D_{V90} (μm)	7.0 (February 2005)	47.6 (January 2006)	28.8 (12.8)
$b_p(555)$ (m^{-1})	≤1.0 (twice in August 2005)	53.1 (January 2005)	6.96 (10.3)
$a_p(440)$ (m^{-1})	0.14 (December 2005)	6.19 (July 2005)	0.76 (1.13)
$a_p(675)$ (m^{-1})	0.044 (February 2005)	4.54 (July 2005)	0.35 (0.78)
$a_{CDOM}(440)$ (m^{-1})	0.023 (April 2005)	0.31 (January 2005)	0.092 (0.054)

[a]December 2004 to June 2006.
[b]The annual average values are accompanied with the standard deviation values in parentheses.

of D_{V50} were typically observed in winter months when POC/SPM was relatively low and particle assemblages were dominated by minerogenic fraction. Larger values of D_{V50} were typical during summer when the POC/SPM was relatively high which suggests a high contribution of organic particles. The size parameter, D_{V90}, representing the 90th percentile of particle volume size distribution, varied between 7 and 48 μm. The D_{V90} data indicate that the contribution of particles larger than 50 μm to the total particle volume was always less than 10%. The percent contributions of these large particles to the total particle abundance and the total particle projected area were even smaller (data not shown).

[29] The large variability observed in the concentrations and composition of seawater constituents at the IBP location resulted in correspondingly large variability in the inherent optical properties (IOPs) of seawater (Table 1). For example, the particulate scattering coefficient b_p at 555 nm showed more than 50-fold variation. At a few experiments (Exp. 23 and 25 in August 2005), the $b_p(555)$ values were below the detection limit of our measurement method (< 1 m^{-1}). There was about 44-fold variation in the particulate absorption coefficient at 440 nm and more than 100-fold variation at 675 nm. Both b_p and a_p exhibited strong covariation with each other, and with indicators of particle concentration such as SPM or $C_v^{2-60\mu m}$.

[30] In contrast to b_p and a_p, the absorption coefficient of CDOM, a_{CDOM}, did not show any consistent covariation with characteristics of the particle assemblage and the range of variation was much less than that of particle absorption. For example, the variation of $a_{CDOM}(440)$ in our study was about 13-fold (Table 1). For the majority of our samples, CDOM had a smaller contribution to absorption than suspended particles in the visible region of the spectrum. Because our primary interest in the present manuscript is to address relationships between particle IOPs and characteristics of the particle assemblage, no further discussion of CDOM absorption is provided in the remainder of the paper.

3.2. Size Distributions and Composition of Particulate Matter

[31] Four distinctly different examples of PSDs for the IBP samples are shown in Figure 1 in terms of density func-

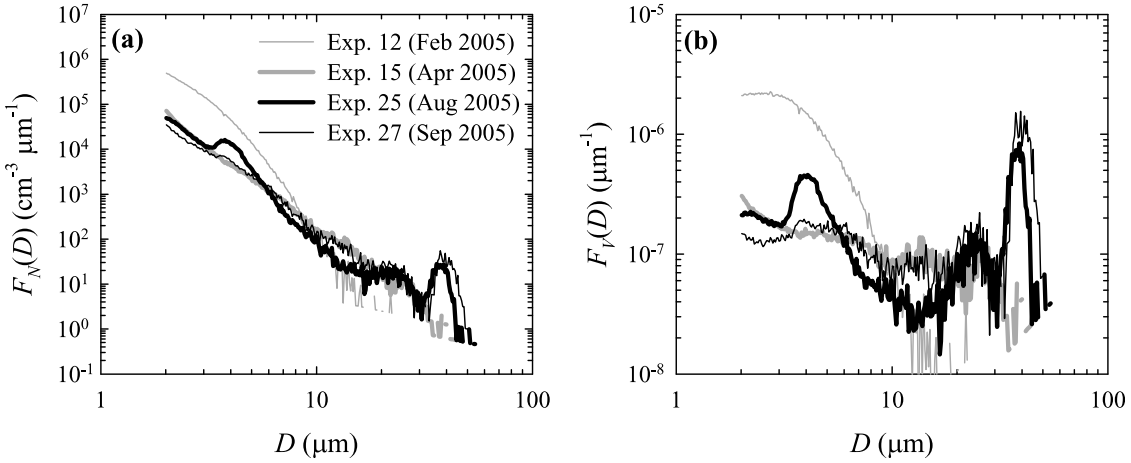

Figure 1. Example particle size distributions for samples collected during several experiments at the Imperial Beach Pier: (a) the density function of particle number concentration, $F_N(D)$, and (b) the density function of particle volume concentration, $F_V(D)$, as functions of particle equivalent spherical diameter, D. Some noise in the data is seen at relatively large values of D (> 10 μm), which is associated with relatively low particle counts within narrow size bins in that diameter range.

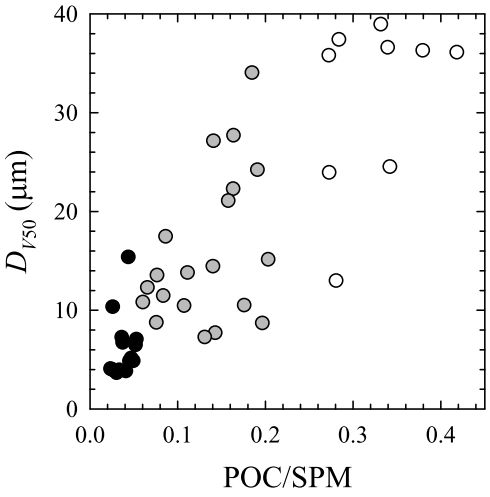

Figure 2. Scatter plot between the median particle diameter, D_{V50}, and the ratio of POC/SPM for the Imperial Beach samples. The mineral-dominated samples are shown as solid circles, the organic-dominated samples as open circles, and the mixed samples as grey circles.

tions for particle number concentration $F_N(D)$ and particle volume concentration $F_V(D)$. Some "high-frequency" noise seen in these data due to limited particle counts within individual size bins, especially for $D > 10$ μm, should be ignored when interpreting these distributions. The sample from Exp. 12 (February 2005) shows a rather featureless $F_N(D)$ with relatively steep local slopes at particle diameters $D <$ 10 μm, albeit with some curvature as well. That sample is also characterized by the smallest value of $D_{V50} = 3.7$ μm among the IBP samples, which indicates the largest contribution of small-sized particles. The $F_N(D)$ distribution for Exp. 15 (April 2005) is also rather featureless but the slopes are generally less steep across the examined size range. The two other examples show clear maxima in particle size distribution, which can be attributed to specific plankton populations. The PSDs for Exp. 25 and 27 (August and September 2005) display a clear maximum around $D = 40$ μm. The secondary maximum, which is more pronounced in Exp. 25 than Exp. 27, is observed at D of about 4 μm. These features are particularly well-defined in the particle volume distribution, $F_V(D)$. We also note that the sample from Exp. 27 had the largest D_{V50} of about 39 μm, and had the greatest contribution of relatively large particles among all samples examined.

[32] Figure 2 is a scatter plot depicting the particle size parameter D_{V50} versus the POC/SPM ratio. This plot has particular significance because we use these two quantities as simple metrics for the key particle characteristics of size and composition, both of which affect the particle IOPs. An important observation for our study site is that the proportion between small-sized and large-sized particles shows a significant degree of covariation with the contribution of POC to SPM. In general, however, there is no reason to expect a consistent well-behaved relationship between the particle size and composition in various aquatic environments. This is because the patterns between these particle characteristics will depend on many factors playing different roles in different environments, such as sources and sinks of particles, particle dynamics, etc.

[33] One important rationale for characterizing composition of particulate matter in optical studies is that the refractive index of particles is dependent on their composition. At visible light wavelengths, the range of refractive index relative to water for phytoplankton cells is 1.06 ± 0.04 [*Aas*, 1996]. Mineral particles generally have significantly higher refractive index; typical values relative to water are within the range 1.12–1.22 for many common mineral species [*Kerr*, 1977]. Therefore, one can expect that the empirical relationships between IOPs and measures of particle concentration or size will improve if established for separate classes of data, each constrained by particulate composition.

[34] We partition the IBP samples into three composition-related groups based on the POC/SPM ratio, and this classification is used throughout the remainder of the paper. The samples with POC/SPM < 0.06 are classified as low POC/SPM and the samples with POC/SPM > 0.25 as high POC/SPM. The remaining samples are classified as intermediate POC/SPM. For convenience, these three groups will be referred to as mineral-dominated, organic-dominated, and mixed, respectively. Although we have not measured the concentrations of POM and PIM, these descriptive terms provide a useful approximate designation of the composition of particulate matter in terms of organic and inorganic contributions. This naming scheme has no adverse effect on the analysis and interpretation of our results, and is justified because POC constitutes a significant fraction of POM, regardless of possible variation in the composition of organic matter. Although the POC/POM is variable and poorly characterized for natural assemblages of particulate matter in coastal environments, a useful insight is provided from studies of organic composition of marine phytoplankton. For example, the traditional Redfield formula implies that carbon contributes about 36% to the organic dry mass of phytoplankton [*Redfield et al.*, 1963]. A range of contributions from about 50% to 60% was suggested on the basis of modified Redfield formula with lower oxygen and hydrogen contents [*Anderson*, 1995]. Some variation in the composition of organic particulate matter during our experiments is indicated by the POC/PON ratio, where PON is the concentration of particulate organic nitrogen. The average POC/PON (by weight) for all IBP samples is 6.39 (SD = 1.64). For the low POC/SPM samples (i.e., mineral-dominated), the average POC/PON = 6.40 (SD = 1.45), and for the high POC/SPM samples (i.e., organic-dominated) the average POC/PON = 8.19 (SD = 2.00). These average values are somewhat higher than the Redfield POC/PON ratio that is about 5.7 (by weight). From these considerations we estimate that our samples with POC/SPM < 0.06 can be expected to have less than 20% contribution of POM to SPM. The samples with POC/SPM > 0.25 can be expected to have POM/SPM > 40%, or probably even > 50%. We also note that the critical POC/SPM values of 0.06 and 0.25 selected for our classification are consistent with clear differences in the patterns of our data partitioned with these POC/SPM values (e.g., differences in the shape of PSD and the spectral shapes of $a_p(\lambda)$ and $b_p(\lambda)$ as illustrated below). A small change in these values would not, however, affect significantly the analysis and main conclusions of this study.

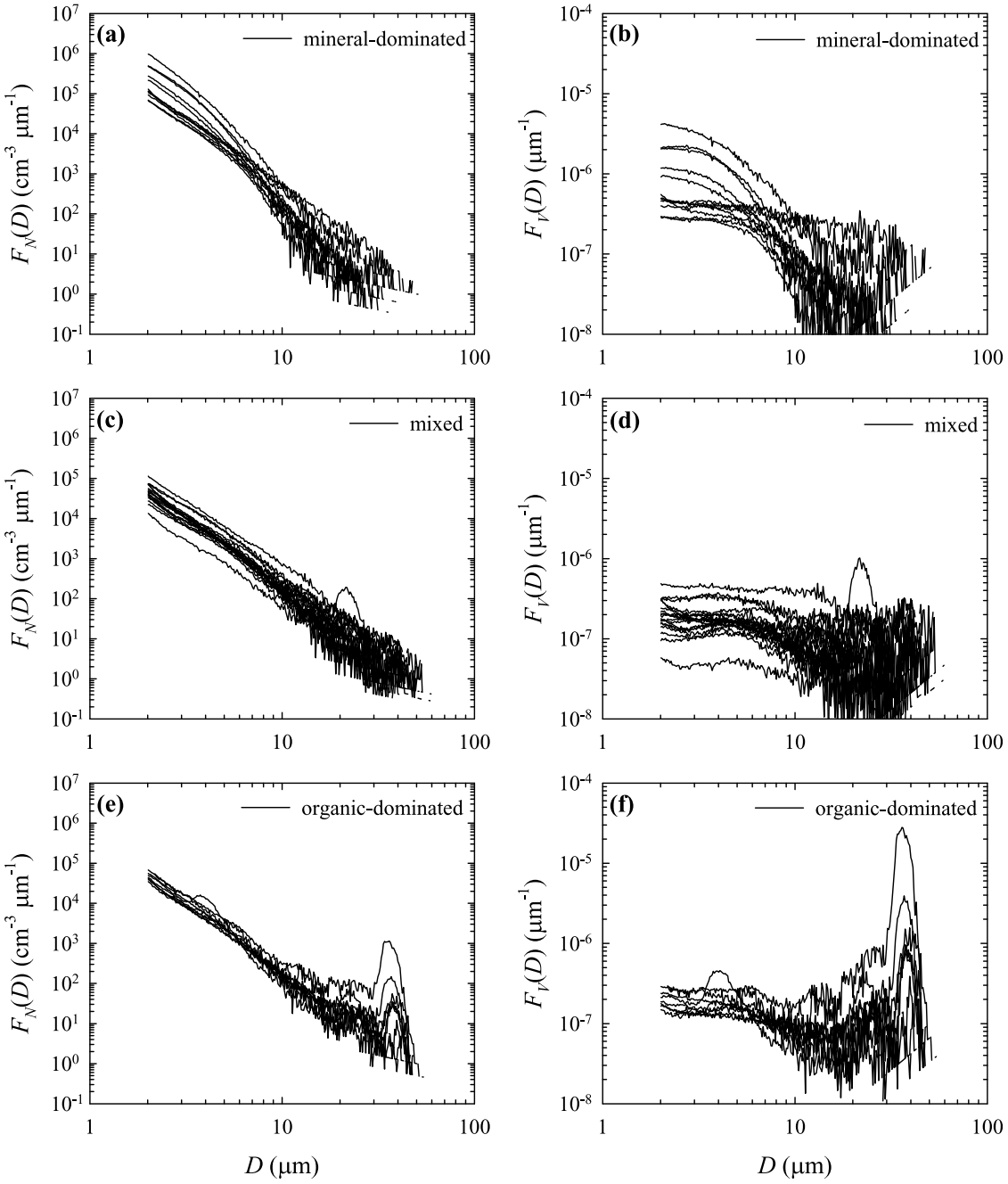

Figure 3. Particle size distributions for all Imperial Beach samples presented in form of (a, c, and e) the density function of particle number concentration $F_N(D)$ and (b, d, and f) the density function of particle volume concentration $F_V(D)$. The distributions for mineral-dominated, mixed, and organic-dominated cases are presented separately in the top, middle, and bottom plots, respectively. Small-scale irregularities represent measurement noise.

[35] Figure 2 shows that mineral-dominated samples have typically smaller values of D_{V50}, and thus larger contribution of small-sized particles compared with organic-dominated samples. Thirteen out of fifteen samples classified as mineral-dominated had the lowest values of D_{V50} smaller than 7.5 μm. In contrast, six out of nine samples classified as organic-dominated had the largest values of D_{V50} exceeding 35 μm. This covariation is of great consequence to the analysis of our optical data because both the particle size distribution and particulate composition are important determinants of particulate IOPs.

[36] Distinct differences in particle size distributions between the mineral-dominated and organic-dominated samples are also evident when comparing the plots of $F_N(D)$ and $F_V(D)$ for all measurements. Whereas the distributions of mineral-dominated samples are always featureless (Figures 3a and 3b), those for organic-dominated or mixed samples often show a large maximum around D = 40 μm

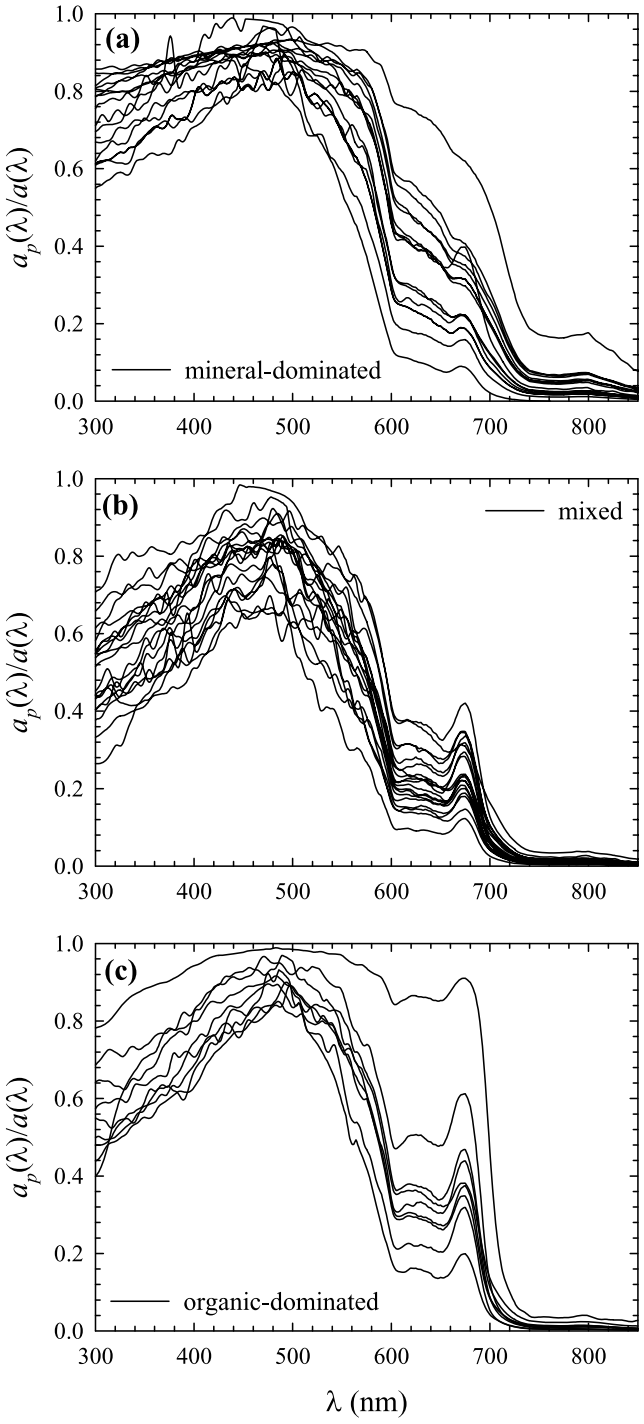

Figure 4. Spectra showing the contribution of particulate absorption, $a_p(\lambda)$, to total absorption coefficient, $a(\lambda)$, for Imperial Beach samples presented separately for: (a) the mineral-dominated; (b) mixed; and (c) organic-dominated cases. Small-scale irregularities represent measurement noise.

(Figures 3e and 3f). In addition, the PSD for mineral-dominated samples is generally steeper than that for organic-dominated samples, which is particularly noticeable in the $F_V(D)$ distributions. When mineral particles dominate, the contribution to the total particle volume shows a clear decreasing trend with an increasing particle diameter. This trend is not evident for organic-dominated samples. In this case the particle volume is more evenly distributed along the examined range of particle diameters, albeit the 10–30 μm range generally makes a somewhat reduced contribution. Also, a major contribution for some organic-dominated samples is associated with a maximum near 40 μm. The mixed samples also exhibit the $F_V(D)$ distributions with similar contributions coming from different particle sizes, especially in the range of $D < 10$ μm (Figure 3d).

3.3. Absorption by Suspended Particles

[37] Suspended particles are a major light absorbing component of the nearshore waters at the IBP location (Figure 4). Regardless of particle composition parameterized in terms of POC/SPM, the absorption by particles for most samples provided a dominant contribution (> 50%) to the total absorption coefficient at light wavelengths shorter than about 550 nm. At longer wavelengths, the contribution of particles decreases because a decrease in the particulate absorption coefficient with light wavelength is accompanied by a steep increase in pure water absorption coefficient. Because of methodological issues related to measurements on bleached sample filters (section 2.4), the partitioning of particulate absorption into phytoplankton and nonphytoplankton components can be addressed only for the organic-dominated IBP samples. For these samples, the ratio of $a_d(\lambda)/a_p(\lambda)$ was generally small at wavelengths between 300 and 700 nm, i.e., within the spectral range where the values of both coefficients were high enough to calculate a meaningful ratio. For example, the average value of a_d/a_p is 0.37 (SD = 0.08) at 350 nm, 0.19 (SD = 0.08) at 440 nm, and 0.23 (SD = 0.10) at 580 nm. These results indicate that most of particulate absorption of organic-dominated samples was caused by phytoplankton pigments.

[38] Figure 5 shows spectra of mass-specific absorption coefficient of particles, $a_p^*(\lambda)$. This coefficient was obtained by normalizing the $a_p(\lambda)$ values to SPM. As expected, the $a_p^*(\lambda)$ spectra for mineral-dominated samples show no or weak signature of major phytoplankton absorption bands centered around 440 nm and 675 nm (Figure 5a). In contrast, these features are easily discernible in the spectra for mixed and organic-dominated samples (Figures 5b and 5c). The $a_p(440)/a_p(400)$ ratio quantitatively describes these differences. Whereas the average ratio is 0.74 (SD = 0.05) for mineral-dominated cases, it is 0.96 (SD = 0.08) and 0.96 (SD = 0.06) for mixed and organic cases, respectively.

[39] The range of variability in the values of $a_p^*(\lambda)$ is quite large at all wavelengths but it is similar for the three groups of IBP samples; the mineral-dominated, the organic-dominated, and the mixed samples. With a few exceptions, the $a_p^*(\lambda)$ values within the visible spectral range (400–680 nm) fall within the range of 0.01 to 0.1 $m^2\ g^{-1}$. The largest variability among the samples is observed in the red band of chlorophyll *a* absorption at about 675 nm (~9.3-fold, CV = 45 % where CV is the coefficient of variation calculated as a ratio of the standard deviation to the mean value and expressed in percent). The smallest but still large variation occurs around 400 nm (~2.9-fold, CV = 25%) and 555 nm (~3.6-fold, CV = 26%), where the influence of phytoplankton pigments is smaller. These two bands are the best candidates for establishing empirical relationships between

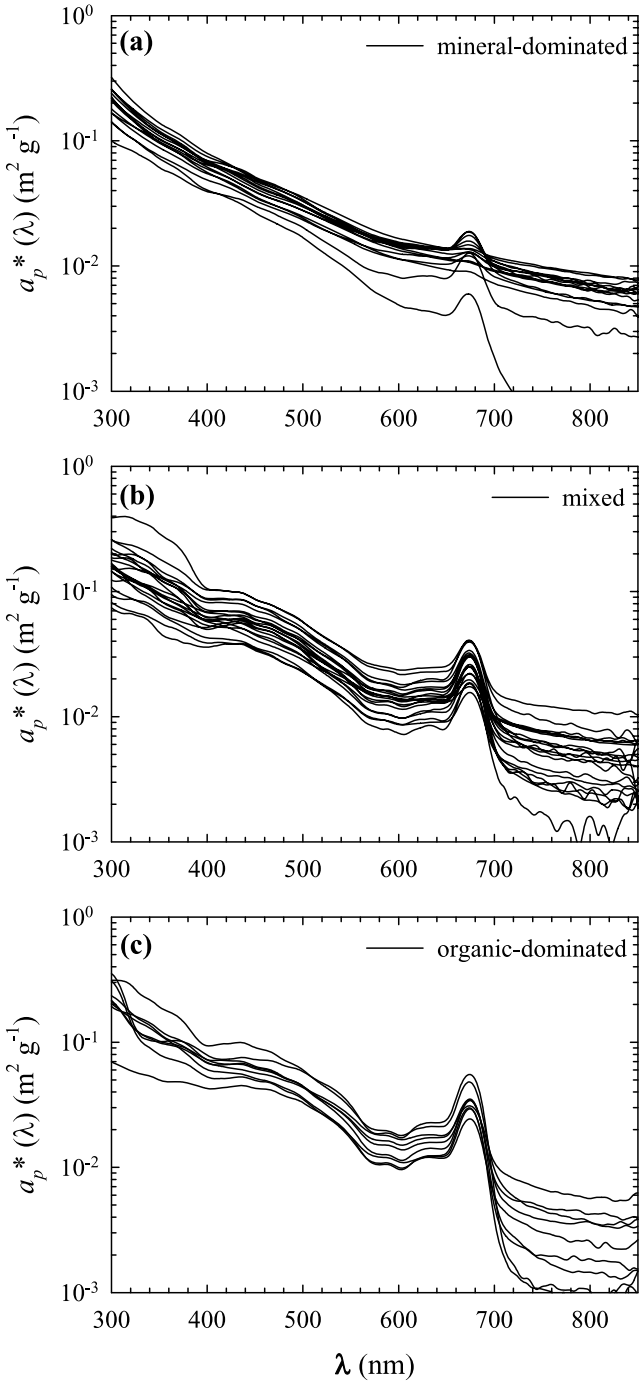

Figure 5. Spectra of mass-specific absorption coefficient of particles, $a_p^*(\lambda)$, for all Imperial Beach samples presented separately for: (a) the mineral-dominated; (b) mixed; and (c) organic-dominated cases.

the absorption and the SPM concentration. Such analysis for 400 nm is presented in Figure 6.

[40] There is a reasonably good relationship between $a_p(400)$ and SPM for all data considered together (Figure 6a). The scatter in the data points and nonlinearity in the trend line suggests some variation in the mass-specific absorption, $a_p^*(400)$. Figure 6b shows the range of variation in $a_p^*(400)$ among individual data points. This range is constrained to significant degree and is similar regardless of the particulate composition. For all IBP samples the average value of $a_p^*(400)$ is 0.064 m^{2}g^{-1} (SD = 0.016 m^{2}g^{-1}). For mineral-dominated samples, the average $a_p^*(400)$ is 0.061 m^{2}g^{-1} (SD = 0.012 m^{2}g^{-1}) and for organic-dominated samples 0.068 m^{2}g^{-1} (SD = 0.015 m^{2}g^{-1}). For the 555 nm band (data not shown), the average value for $a_p^*(555)$ is 0.019 m^{2}g^{-1} (SD = 0.005 m^{2}g^{-1}) based on all IBP samples.

[41] Although some contribution to the observed variability in $a_p^*(\lambda)$ can be associated with unavoidable uncertainties in measuring $a_p(\lambda)$ and SPM, the major effects are expected to arise from natural variations in the composition and size distribution of particulate matter. Because Figure 6b does not show a clear trend or relation between $a_p^*(400)$ and particulate composition, it is of particular interest to examine the potential relationship between a_p^* and particle size characteristics. Figure 6c shows $a_p^*(400)$ versus the median particle diameter D_{V50}. The data representing the mineral-dominated and organic-dominated cases are clearly separated. Despite some scatter in the data points, a trend of a decrease in $a_p^*(400)$ with increasing D_{V50} is seen within each class of particle composition. This trend is most evident for mineral-dominated samples. A decrease in the chlorophyll *a*-specific absorption with an increase in cell size has long been recognized as the so-called package effect in phytoplankton [*Morel and Bricaud*, 1981]. Qualitatively similar effect of a decrease in the mass-specific absorption with an increase in particle size was also reported in a modeling study of mineral particles [*Woźniak and Stramski*, 2004] and laboratory measurements of mineral-rich particulate matter [*Stramski et al.*, 2007]. The pattern displayed by the data in Figure 6c is thus consistent with those previous studies.

[42] Our absorption data for mineral-dominated samples are also generally in good agreement with previous field measurements of natural particulate assemblages in marine environments presumably dominated by minerogenic particles [*Bowers et al.*, 1996; *Babin et al.*, 2003b; *Bowers and Binding*, 2006; *McKee and Cunningham*, 2006]. *Bowers and Binding* [2006] analyzed several data sets and concluded that the average spectrum of $a_p^*(\lambda)$ for mineral particles can be approximated with an exponential function: $a_p^*(\lambda) = C_1 + C_2 \exp[(-S_p(\lambda - \lambda_{ref})]$. The best fit parameters were C_1 = 0.020 m^2 g^{-1} (SD = 0.005 m^2 g^{-1}), C_2 = 0.042 m^2 g^{-1} (SD = 0.012 m^2 g^{-1}), S_p = 0.012 nm^{-1} (SD = 0.002 nm^{-1}), and the reference wavelength λ_{ref} is around 440 nm (either 440 nm or 443 nm). It is noteworthy that the estimate of parameter C_1, which represents the background absorption at long wavelengths, is in agreement with the $a_p^*(\lambda)$ values in the near-IR for several mineral-rich samples examined in the laboratory study of *Stramski et al.* [2007]. The sum of C_1 and C_2 yields an average estimate of $a_p^*(440)$ = 0.062 m^2 g^{-1}. In the present study, the average value of $a_p^*(440)$ is 0.057 m^2 g^{-1} (SD = 0.017 m^2 g^{-1}) based on all IBP samples treated together regardless of particulate composition. If the three groups of IBP samples are considered separately, then we have $a_p^*(440)$ = 0.045 m^2 g^{-1} (SD = 0.008 m^2 g^{-1}), 0.062 m^2 g^{-1} (SD = 0.018 m^2 g^{-1}), and 0.065 m^2 g^{-1} (SD = 0.015 m^2 g^{-1}) for mineral-dominated, mixed, and organic-dominated cases, respectively. The average slope S_p of the particulate absorp-

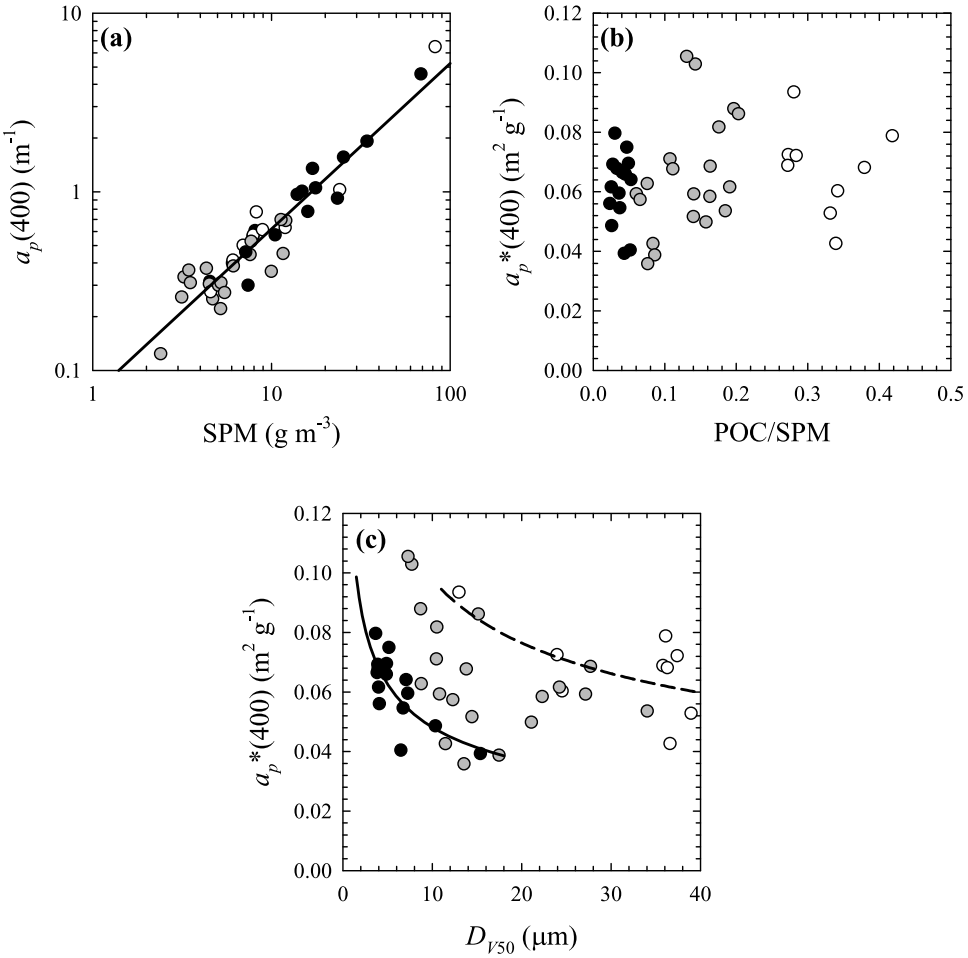

Figure 6. (a) Relationship between the absorption coefficient of particles, $a_p(400)$, and SPM. (b) Scatter plot for the mass-specific absorption coefficient, $a_p^*(400)$, vs. POC/SPM. (c) The mass-specific absorption coefficient of particles, $a_p^*(400)$, vs. particle size parameter, D_{V50}, for the Imperial Beach samples. The IBP data are designated as solid circles for mineral-dominated samples, open circles for organic-dominated samples, and grey circles for mixed samples. The solid line in Figure 6a represents the best fit power function $a_p(400) = 0.0732\ (\mathrm{SPM})^{0.927}$ (the r^2 coefficient between the log-transformed data is 0.89, number of observations $n = 44$). The linear function (not shown) yields $r^2 = 0.96$ (or 0.97 if the fit is forced to have zero offset) but the mean normalized bias and root mean square errors are somewhat higher compared with the power function fit. Two power function fits presented in Figure 6c are: $a_p^*(400) = 0.115\ (D_{V50})^{-0.378}$ (solid line) for mineral-dominated samples, and $a_p^*(400) = 0.222\ (D_{V50})^{-0.356}$ (dashed line) for organic-dominated samples. The r^2 values between the log-transformed data are 0.57 and 0.32, and the number of observations $n = 15$ and 9, respectively.

tion spectra for IBP samples dominated by minerals is 0.0119 nm^{-1} (SD = 0.0016 nm^{-1}), which is also in good agreement with S_p determined by *Bowers and Binding* [2006]. Our determinations of S_p are based on the spectral range 300–800 nm.

3.4. Scattering by Suspended Particles

[43] Figure 7 shows spectra of the mass-specific scattering coefficient of suspended particles, $b_p^*(\lambda)$, for the mineral-dominated, mixed, and organic-dominated samples. The $b_p^*(\lambda)$ values were determined as a ratio of $b_p(\lambda)$ to SPM. As was the case with the absorption data, the small-scale irregularities seen in the scattering spectra are again mostly attributable to measurement noise rather than real spectral features. The general spectral trend and the magnitude of scattering are, however, well revealed by our data. As seen, the scattering spectra typically display an increase towards shorter light wavelengths but in some cases the data show very little or no wavelength dependence. The magnitude of $b_p^*(\lambda)$ varies significantly at all wavelengths, although somewhat less at the long-wavelength end of the spectrum, especially for the mineral-dominated and organic-dominated samples. Overall, however, the range of variation is similar for the three groups of samples with the mineral-dominated cases exhibiting a slightly smaller range compared with the mixed and organic-dominated cases.

[44] If all IBP samples are considered together, the relative variations in the mass-specific scattering $b_p^*(\lambda)$ appear

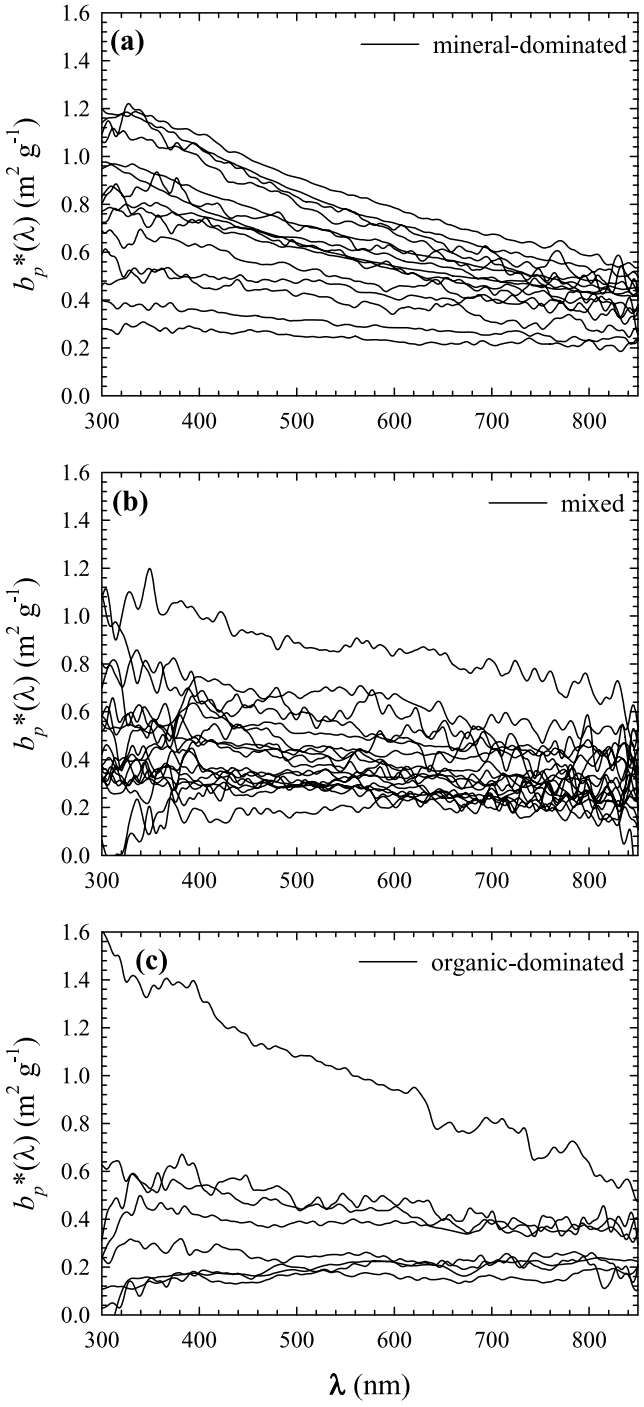

Figure 7. Spectra of mass-specific scattering coefficient of particles, $b_p^*(\lambda)$, for all Imperial Beach samples presented separately for (a) the mineral-dominated, (b) mixed, and (c) organic-dominated cases. Note that one spectrum in Figure 7c shows erroneously low scattering values at the shortest UV wavelengths, which is likely attributable to an uncertainty in measuring high optical signal (especially absorption) at these wavelengths for the sample collected during a massive phytoplankton bloom. Small-scale irregularities represent measurement noise.

to be larger than the relative variations observed in the mass-specific absorption $a_p^*(\lambda)$. This is especially true for the wavelengths of 400 nm and 555 nm, where absorption showed the smallest range of variability. As a result, the correlation between the particulate scattering b_p and SPM (Figure 8a) is not as strong as that for a_p vs. SPM. The scatter plot of $b_p^*(555)$ vs. POC/SPM in Figure 8b illustrates the relatively wide range of variation in $b_p^*(555)$ among individual data points. The entire IBP data set yields an average value of $b_p^*(555) = 0.47$ m^{2}g^{-1} (SD = 0.20 m^{2}g^{-1}). The maximum to minimum range is more than 6-fold, and both the minimum $b_p^*(555) = 0.16$ m^{2}g^{-1} and the maximum of 1.01 m^{2}g^{-1} were observed for the organic-dominated samples. This range of variability in b_p^* indicates that the mass-specific scattering provides a less attractive proxy for SPM than the mass-specific absorption coefficients, such as $a_p^*(400)$, for the nearshore waters at the IBP location.

[45] Whereas the scatter in the data points in Figure 8b is quite large, there appears to be a weak tendency of decreasing $b_p^*(555)$ with an increase in POC/SPM. It is interesting to note that most of mineral-dominated samples showed the $b_p^*(555)$ values higher than those for most of organic-dominated samples. For the mineral-dominated samples, which show the smallest range of variation among the three sample groups examined, the average $b_p^*(555)$ is 0.57 m^{2}g^{-1} (SD = 0.18 m^{2}g^{-1}) and the range is ~3.5-fold (from 0.24 to 0.84 m^{2}g^{-1}). It is also noteworthy that the range of variability in $b_p^*(\lambda)$ decreases with wavelength. For example, in the NIR at 800 nm, the average $b_p^*(800)$ at the IBP location is 0.411 m^{2}g^{-1} (SD = 0.105 m^{2}g^{-1}) for mineral-dominated samples, 0.329 m^{2}g^{-1} (SD = 0.145 m^{2}g^{-1}) for organic-dominated samples, and 0.352 m^{2}g^{-1} (SD = 0.146 m^{2}g^{-1}) for mixed samples.

[46] Because the particle size distribution is an important determinant of scattering, it is of interest to examine the relationship between b_p^* and particle size characteristics (Figure 8c). The values of $b_p^*(555)$ plotted as a function of the median diameter D_{V50} show a general decrease of b_p^* with D_{V50} and the data representing the mineral-dominated and organic dominated samples are clearly separated. A particularly good power function fit holds for mineral-dominated samples. Although the data points for mixed and organic-dominated samples are more scattered, they still support the notion that the particulate assemblages with higher relative contributions of small-sized particles are more likely to be more efficient scatterers per unit mass concentration of particles than the assemblages characterized by relatively greater abundance of larger-sized particles. This conclusion is consistent with Mie scattering modeling [*Babin et al.*, 2003a; *Woźniak and Stramski*, 2004] and laboratory measurements of mineral-rich particulate assemblages suspended in seawater [*Stramski et al.*, 2007; *Stramska et al.*, 2008].

[47] The particle size distribution also exerts a significant influence on the spectral behavior of particulate scattering. To examine this effect we fitted a power function $b_p(\lambda) \sim \lambda^{\eta}$ (where η is the slope parameter) to the $b_p(\lambda)$ data within the wavelength range of 400–800 nm. We found that the mineral-dominated samples showed the strongest dependence on light wavelength with an average slope $\eta = -0.80$ (SD = 0.19). The spectral slope for the mixed samples was, on average, −0.49 (SD = 0.33) and for organic-

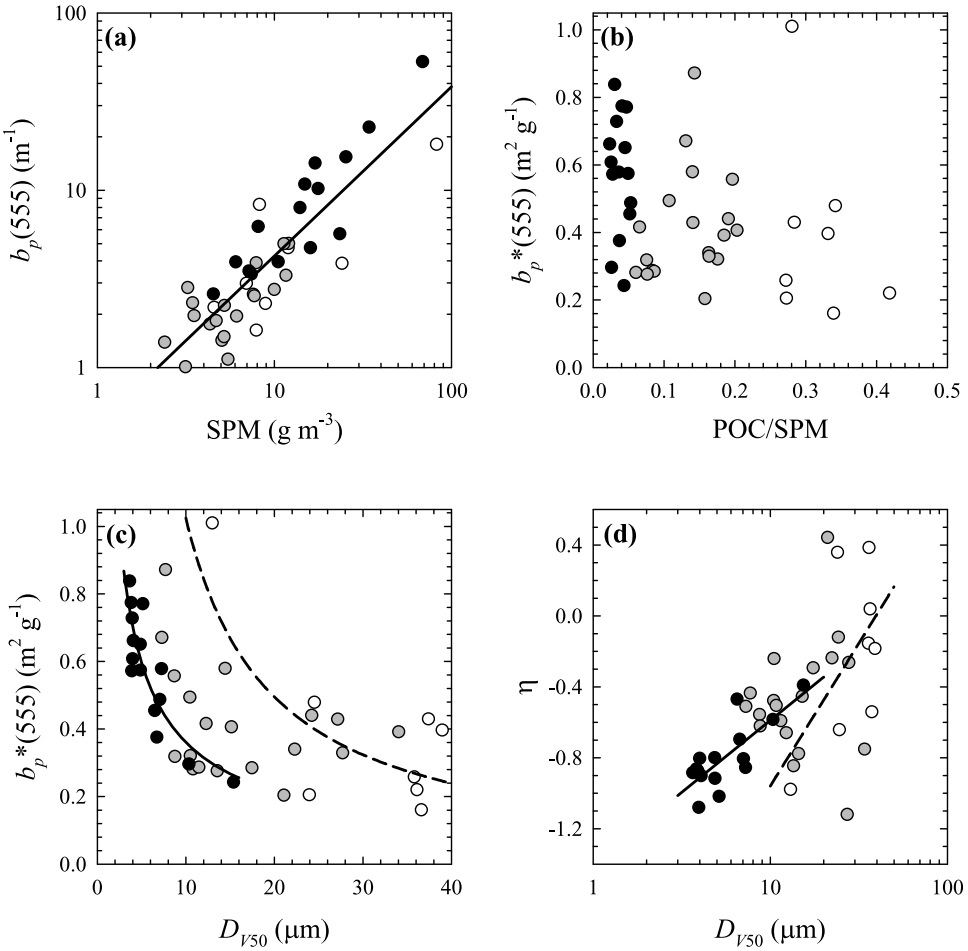

Figure 8. (a) Relationship between the scattering coefficient of particles, $b_p(555)$, and SPM. (b) Scatter plot between the mass-specific scattering coefficient of particles, b_p*(555), and POC/SPM ratio. (c) The mass-specific scattering coefficient of particles, b_p*(555), and particle size parameter, D_{V50}. (d) The spectral slope of particulate scattering, η, and particle size parameter, D_{V50}, for the Imperial Beach samples (coding of data points as in Figure 6). The solid line in Figure 8a represents the best fit power function $b_p(555) = 0.472\ (\mathrm{SPM})^{0.955}$ (the r^2 value between the log-transformed data is 0.74, number of observations $n = 42$). The linear function (not shown) provides a similarly good fit ($r^2 = 0.65$ or 0.77 if the fit is forced to have zero offset). For mineral-dominated and organic-dominated samples the best regression fits to the data are shown in Figures 8c and 8d. For the mineral-dominated samples (solid lines), the regression equations are: b_p*(555) = 2.09 $(D_{V50})^{-0.784}$ (the r^2 between the log-transformed data is 0.82, and the number of observations $n = 15$) and $\eta = 0.352\ \ln(D_{V50}) - 1.4$ (the r^2 between the log-transformed variable of D_{V50} and variable of η is 0.60, $n = 15$). For the organic-dominated samples (dashed lines) the equations are b_p*(555) = 11.5 $(D_{V50})^{-1.05}$ and $\eta = 0.699\ \ln(D_{V50}) - 2.57$ ($r^2 = 0.45$ and 0.30, respectively, and $n = 8$).

dominated samples −0.22 (SD = 0.48). These changes in η are consistent with variations in particle size distribution parameterized in terms of D_{V50} (Figure 8d). As the role of larger particles becomes more important with an increasing role of organic particles (see Figure 2), the slope becomes flatter and the scattering spectra of organic-dominated samples become less dependent on λ as compared with the mineral-dominated samples.

[48] Previously published values of the mass-specific scattering of marine particles based on field experiments also show a significant degree of variation. *Babin et al.* [2003a] reported that b_p*(555) is typically about 0.5 $m^2 g^{-1}$ in various coastal waters around Europe. On the basis of theoretical considerations they suggested that such magnitude of b_p*(555) is explainable by the dominant presence of mineral particles, which are characterized by low or negligible water content, high particle density, and relatively high refractive index. The effects of an increase in particle density and refractive index on b_p* counterbalance one another, as the former leads to a decrease and the latter to an increase of b_p*. As shown above, the magnitude of b_p* is also sensitive to the particle size distribution. *Babin et al.* [2003a] suggested that the values of 0.5 $m^2 g^{-1}$ can be expected as typical for mineral-dominated assemblages that obey approximately a Junge-type size distribution with a slope of about −4. In another recent study of coastal waters within

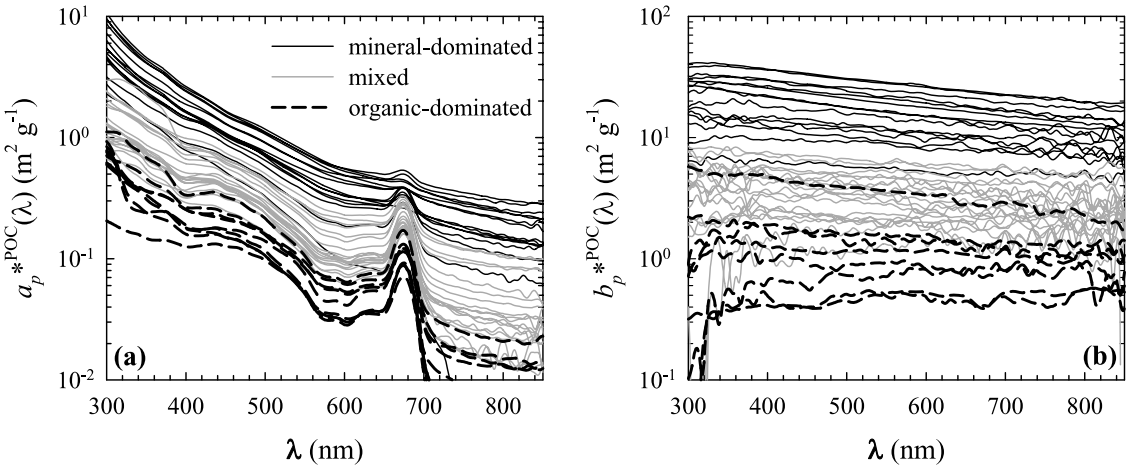

Figure 9. Spectra of (a) POC-specific absorption coefficient of particles, $a_p{}^{*POC}(\lambda)$ and (b) POC-specific scattering coefficient of particles, $b_p{}^{*POC}(\lambda)$, for all Imperial Beach samples. The spectra for mineral-dominated samples are shown as solid black lines, for organic-dominated samples as dashed lines, and for the mixed samples as solid grey lines. Small-scale irregularities in the spectra represent measurement noise.

the northern Gulf of Mexico, *Stavn and Richter* [2008] reported the mass-specific scattering coefficient for the inorganic fraction of particulate matter in the range 0.6–0.69 m^2g^{-1} (at 555 nm). We recall that the average value of b_p*(555) for our entire IBP data set is 0.47 m^2g^{-1} and for the mineral-dominated samples is 0.57 m^2g^{-1}.

[49] It is also of interest to bring to attention the result of *Babin et al.* [2003a] for open ocean waters in the Atlantic. In these waters they observed relatively high values of b_p* (555) of ~1 m^2g^{-1}, which are twice as high as their typical estimates in coastal waters. The explanation for the open ocean waters offered on the basis of Mie scattering calculations involved the dominant role of organic particles that have significant water content and low apparent density. Our data from the nearshore marine environment show that the organic-dominated particulate assemblages can produce a broad range of b_p* from less than 0.2 m^2g^{-1} to above 1 m^2g^{-1}, largely in response to changes in particle size distribution (Figure 8c). The determinations of mass-specific scattering for the organic fraction of particulate matter in the Gulf of Mexico by *Stavn and Richter* [2008, Figures 3 and 5] also show that this coefficient can be significantly higher or lower than 1 m^2g^{-1}. These results caution against indiscriminate assumption that organic-dominated waters will typically have higher values of b_p* than mineral-dominated waters. In our IBP data set, the b_p* for organic-dominated samples is actually often times lower than for mineral-dominated samples.

3.5. POC-Specific Optical Coefficients

[50] Recent studies have shown that optical measurements can serve as a proxy for POC concentration in seawater, especially in the open ocean where organic constituents are a primary source of optical variability [e.g., *Loisel and Morel*, 1998; *Stramski et al.*, 1999, 2008; *Gardner et al.*, 2006]. Whereas the earlier studies recognize that the relationships between POC and optical properties will deteriorate in marine environments that are largely affected by inorganic constituents (e.g., many coastal waters), the extent of this problem has not yet been quantified with an adequate set of systematically collected data in such environments. Our data from the IBP location allows us to address this problem.

[51] Figure 9 shows the spectra of POC-specific absorption and scattering coefficients, $a_p{}^{*POC}(\lambda)$ and $b_p{}^{*POC}(\lambda)$ respectively, for the IBP samples. These coefficients are defined as a ratio of $a_p(\lambda)$ and $b_p(\lambda)$ to POC concentration. As could be expected for waters with large variation in particulate composition, both $a_p{}^{*POC}(\lambda)$ and $b_p{}^{*POC}(\lambda)$ show a very large variation with the highest values observed for mineral-dominated samples (low POC/SPM) and the lowest values for the organic-dominated samples (high POC/SPM). The range of $a_p{}^{*POC}(\lambda)$ spans more than one order of magnitude and the range of $b_p{}^{*POC}(\lambda)$ as much as two orders of magnitude. The smallest range of variability observed for $a_p{}^{*POC}(675)$ is still characterized by large coefficient of variation of 51% around the average value of $a_p{}^{*POC}(675)$ = 0.25 m^2g^{-1}. Thus, our IBP data set indicates that the bulk IOP coefficients cannot serve as adequate direct proxies for estimating POC in marine environments where particulate composition varies over a broad range. However, Figure 9 also suggests that improvement can be achieved if each of the three categories of particulate composition is considered separately. For example, the coefficient of variation of $a_p{}^{*POC}$ at 400 nm or 675 nm is reduced to ~30% for each composition group of data considered separately.

3.6. Estimation of Particulate Characteristics From IOPs

[52] Optical measurements have long been recognized as an attractive approach for estimating various characteristics of seawater constituents, which are of interest to a range of problems in aquatic ecology, biogeochemistry, and water quality. A major benefit results from the fact that in situ or remote (airborne or spaceborne) optical sensors provide a capability for measurements over extended spatial and temporal scales, which are not accessible to analytical techniques applied to discrete water samples. The variability in the data presented above supports, however, the notion

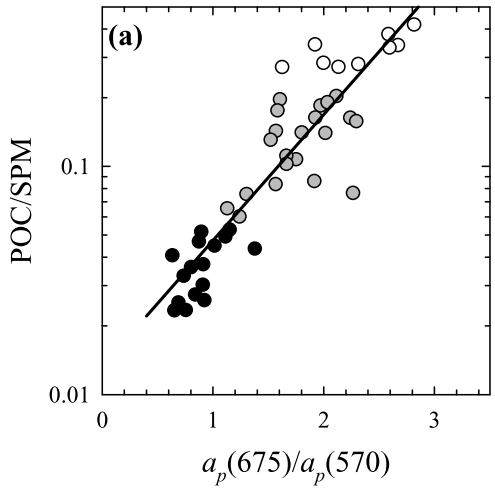

Figure 10. Relationship between the POC/SPM ratio and the spectral ratio of the particulate absorption coefficients, $a_p(675)/a_p(570)$, for the Imperial Beach samples (coding of data points as in Figure 6). The regression line plotted is: POC/SPM = 0.0133 exp{1.27[$a_p(675)/a_p(570)$]}. The r^2 value between the log-transformed variable of POC/SPM and the variable of $a_p(675)/a_p(570)$ is 0.81. The number of observations n = 44.

that estimating characteristics of suspended particulate matter from optical measurements is highly challenging, especially in optically complex marine environments such as nearshore waters. Here we illustrate an example approach for building empirical algorithms for estimating particulate characteristics from measured IOPs in such complex environments, using relationships established with our IBP data set. Because this example is based on a relatively small number of data collected at the single location, we deter from emphasizing the predictive or operational significance of the presented algorithm. This presentation is instead used primarily to demonstrate the conceptual approach of how measurements of particulate IOPs can be used to estimate characteristics of particulate composition (POC/SPM), particle size distribution (D_{V50}), and particle concentration (SPM and POC).

[53] The main underlying idea of the approach is that the empirical relationships between the IOPs and the metrics of particle concentration and size are established separately for distinct groups of data representing different particulate composition. Therefore, as a first step, a metric of particulate composition must be estimated from measured IOPs. For this purpose, we tested relationships between POC/SPM and several IOP ratios. For example, we found reasonably good relationships between POC/SPM and the following IOP ratios: $a_p(675)/b_p(675)$, $a_p(480)/a_p(570)$, and $a_p(675)/a_p(570)$. The latter provided a slightly better predictor of POC/SPM than the other IOP ratios. The relationship between POC/SPM and $a_p(675)/a_p(570)$ for the entire set of IBP data is (see also Figure 10)

$$\frac{\mathrm{POC}}{\mathrm{SPM}} = 0.0133\ \exp\left[1.27\frac{a_p(675)}{a_p(570)}\right]. \qquad (1)$$

The squared correlation coefficient r^2 between the log-transformed values of POC/SPM and the data of $a_p(675)/a_p(570)$ is 0.81 (number of observations n = 44). The values of mean normalized bias, MNB, and normalized root mean square error, NRMSE, are 7.4% and 44.7%, respectively. The formulas for calculating MNB and NRMSE can be found elsewhere [e.g., *Stramski et al.*, 2008]. In the following text, the reported values of r^2 correspond either to two log-transformed variables (in the case of power function fits) or one log-transformed and one ordinary variable (exponential fits).

[54] With the POC/SPM estimated from equation (1), several options are available to estimate the remaining parameters, D_{V50}, SPM, and POC. In these determinations we use empirical relationships established separately for the mineral-dominated (POC/SPM < 0.06) and for organic-dominated (POC/SPM > 0.25) samples. For the mineral samples the relationships are typically the best and for the organic samples the relationships are also usually acceptable. For the mixed samples (0.06 ≤ POC/SPM ≤ 0.25), the relationships are inferior and often useless. However, below we provide relationships that allow the estimation of SPM and POC for the mixed samples.

[55] The particle size parameter, D_{V50}, can be estimated from the spectral slope of particulate scattering, η,

for mineral-dominated samples (see data in Figure 8d)

$$D_{V50} = 21.4\ \exp(1.69\ \eta)$$
$$\left(r^2 = 0.6;\ \mathrm{MNB} = 3.3\%,\ \mathrm{NRMSE} = 27\%;\ n = 15\right), \qquad (2a)$$

and for organic-dominated samples

$$D_{V50} = 32.0\ \exp(0.432\ \eta)$$
$$\left(r^2 = 0.3;\ \mathrm{MNB} = 4.7\%,\ \mathrm{NRMSE} = 35.4\%;\ n = 8\right). \qquad (2b)$$

The SPM concentration can be obtained from the particulate absorption coefficient, $a_p(400)$ (see data in Figure 6a) for mineral-dominated samples

$$\mathrm{SPM} = 16.5\ \left[a_p(400)\right]^{0.946}$$
$$\left(r^2 = 0.92;\ \mathrm{MNB} = 1.9\%,\ \mathrm{NRMSE} = 19.4\%;\ n = 15\right), \qquad (3a)$$

for organic-dominated samples

$$\mathrm{SPM} = 14.9\ \left[a_p(400)\right]^{0.954}$$
$$\left(r^2 = 0.93;\ \mathrm{MNB} = 2.2\%,\ \mathrm{NRMSE} = 21.6\%;\ n = 9\right), \qquad (3b)$$

and for mixed samples

$$\mathrm{SPM} = 14.7\ \left[a_p(400)\right]^{0.916}$$
$$\left(r^2 = 0.61;\ \mathrm{MNB} = 4.2\%,\ \mathrm{NRMSE} = 31\%;\ n = 20\right). \qquad (3c)$$

We note that the statistical errors for equations (2)–(3) represent strictly a scenario in which all samples are correctly classified into one of the particulate composition groups from equation (1). In reality, this will not be exactly the case as, for example, a small percentage of mixed samples may be classified as mineral or organic-dominated samples. This may slightly affect the resultant statistical errors for estimating D_{V50} and SPM.

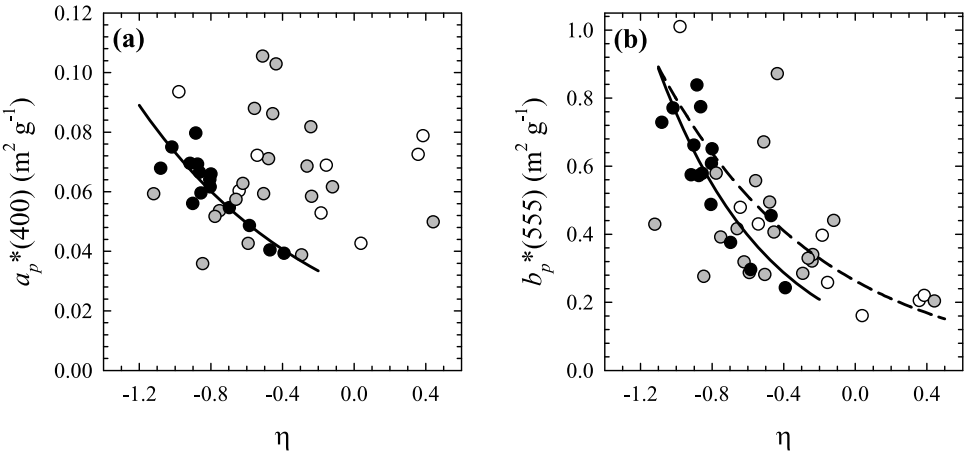

Figure 11. Relationships between (a) the mass-specific absorption coefficient of particles, a_p*(400), and the spectral slope of particulate scattering η and (b) the mass-specific scattering coefficient of particles, b_p*(555), and η, for the Imperial Beach samples (coding of data points as in Figure 6). Three regression lines are also plotted. For the mineral-dominated samples (solid lines in both plots), the regression equations are: a_p*(400) = 0.0275 exp(−0.979η) and b_p*(555) = 0.151 exp(−1.61η), with the r^2 values of 0.80 and 0.72, respectively (the number of observations n = 15). For the case of organic-dominated samples (dashed line in Figure 11b) the regression equation is b_p*(555) = 0.263 exp(−1.11η) and r^2 = 0.81 (n = 8).

[56] The final parameter of interest, the POC concentration, can be simply calculated as

$$\mathrm{POC} = \mathrm{SPM}\,\frac{\mathrm{POC}}{\mathrm{SPM}} \tag{4}$$

using POC/SPM from equation (1) and SPM from an appropriate equation, (3a), (3b), or (3c). This is a two-step algorithm affected by errors in the estimates of both POC/SPM and SPM. The best resultant error statistics for POC estimation were obtained for the mixed samples. In this case, the aggregate statistical parameters of MNB and NRMSE for the composite two-step POC algorithm are 5.6% and 25.2%, respectively (n = 20). For the mineral-dominated samples MNB = 17.1% and NRMSE = 30.3% (n = 15), and for the organic-dominated samples MNB = −17.6% and NRMSE = 30.3% (n = 9). Although these errors, especially MNB, are high in comparison to estimates of other particulate characteristics, the results are encouraging given that the relationships are based on a relatively small number of observations in an optically complex environment.

[57] As an alternative to equations (2a) and (2b), D_{V50} can be estimated from the mass-specific scattering coefficients b_p*(555) (see data in Figure 8c) using the SPM values estimated from equations (3a) and (3b). Because this calculation is a two-step algorithm, these estimates of D_{V50} are expected to be generally less accurate than those obtained in a single step from equations (2a) and (2b).

[58] After calculating POC/SPM from equation (1), another option of the algorithm could begin with the estimation of the mass-specific scattering coefficient from the spectral slope of scattering (see Figure 11)

for mineral-dominated samples

$$b_p^*(555) = 0.151\exp(-1.61\ \eta)$$
$$\left(r^2 = 0.72;\ \mathrm{MNB} = 1.7\%,\ \mathrm{NRMSE} = 18.6\%;\ n = 15\right), \tag{5a}$$

and for organic-dominated samples

$$b_p^*(555) = 0.263\ \exp(-1.11\ \eta)$$
$$\left(r^2 = 0.81;\ \mathrm{MNB} = 3\%,\ \mathrm{NRMSE} = 27.9\%;\ n = 8\right). \tag{5b}$$

It is also interesting that we found a good relationship between the mass-specific absorption and the spectral slope of scattering, but only for the mineral samples (see Figure 11a)

$$a_p^*(400) = 0.0275\ \exp(-0.979\ \eta)$$
$$\left(r^2 = 0.80;\ \mathrm{MNB} = 0.4\%,\ \mathrm{NRMSE} = 9.4\%;\ n = 15\right). \tag{5c}$$

From the relationships (5a), (5b), and (5c), SPM can be calculated as a ratio of the measured coefficients $b_p(555)$ or $a_p(400)$ to the estimated mass-specific coefficients, b_p*(555) or a_p*(400). One of the SPM estimates could be chosen as final or the two or three estimates could be averaged, if deemed to provide a more reliable approximation of the true value of SPM. The POC concentration can then be determined as above from equation (4).

4. Conclusions

[59] Large temporal variability in the concentration and composition of seawater constituents was observed in the nearshore marine environment at Imperial Beach, and led to correspondingly large variability in the inherent optical properties of seawater. Both winter rainstorm events and massive summer phytoplankton blooms produce high turbidity in the investigated waters, with the particulate scattering coefficient exceeding 10 m^{-1} and the particulate absorption coefficient exceeding 1 m^{-1} in the visible spectral region. The minimum values of these coefficients observed generally during dry periods in winter or late spring are below 1 m^{-1} and 0.1 m^{-1}, respectively. Changes

in the particulate assemblage included the dominance of mineral particles with relatively steep particle size distributions during rainstorm events, and the dominance of organic particles with significantly larger contribution of large-sized particles during blooms. These dynamics have important implications to the variability in the magnitude and spectral behavior of IOPs, including the mass-specific absorption and scattering coefficients which underwent several-fold variation in the study area.

[60] In principle, the in-depth mechanistic understanding of such complex optical variability could be addressed through a reductionist approach [*Stramski et al.*, 2001, 2004a], in which the knowledge about optically significant water constituents is available at a significant level of detail for a number of particle functional types that have distinctly different properties and play distinctly different optical and biogeochemical roles in the aquatic environment. Example research efforts in this direction include recent work in which a number of plankton species [*Stramski et al.*, 2001] or several different groups of minerogenic particles [*Peng and Effler*, 2007; *Peng et al.*, 2007] are treated as separate components affecting the bulk IOPs of water. However, a common approach in hydrologic optics over the past decades has been to address the optical variability at a much more general level of water composition parameterization in terms of bulk or aggregate characteristics of suspended particulate matter. Although in this study we have also adopted such a pragmatic approach, we show that as a minimum requirement for advancing an understanding of optical variability in aquatic environments, especially complex coastal waters, the optical measurements must be accompanied not only with the determinations of proxies for bulk particle concentration such as SPM, POC, and Chl, but also particle size distribution and particle composition accounting for separate contributions of organic and inorganic fractions. Admittedly, our determinations of particle size distribution within a size range of 2 to 60 μm represent some limitation, but this can be moderated by improving or combining measurement capabilities in regards to sizing smaller and larger particles. The use of POC/SPM ratio as a proxy for particulate composition could also be enhanced by additional determinations of POM and PIM from the LOI technique [e.g., *Stavn and Richter*, 2008].

[61] One important attribute of optical measurements is that they offer a potential tool for characterizing stocks and dynamics of biogeochemically significant constituents of water over extended temporal and spatial scales of observation. This requires algorithms for converting the optical measurements to water constituent characteristics. The inverse empirical approaches presented briefly in this study are not meant to provide optimum or generalized algorithms, but merely serve as example concepts based on our data from a specific location within a nearshore environment at Imperial Beach. We expect that these example concepts may have broader significance to coastal ocean optics beyond the local character of this study.

[62] The estimation of different particulate characteristics from IOPs will be always subject to unavoidable uncertainties regardless of whether the applied approach is empirical or involves theoretical or semianalytical considerations. For example, the high complexity of natural particulate assemblages involves optically significant particle properties that are not amenable to theoretical treatment, such as the variations in the shape of particles and the internal heterogeneity of particle composition and refractive index. The empirical approaches always exhibit some degree of natural variability and may often require site-specific relationships to ensure acceptable reliability. In this study, some empirical relationships are characterized by a good correlation (mostly those for mineral-dominated samples), but others have a smaller correlation (typically organic-dominated samples) or poor correlation (typically mixed samples). Although this result may to some extent be attributed to the limited size of our data set, an important reason for reduced correlations is certainly associated with the optical complexity and variability of natural particulate assemblages. Nevertheless, the presented examples suggest that the concept of a multistep algorithm, which starts with the estimation of particle composition metric and then uses a set of relationships established separately for different particle composition-related groups of data, promises an improved empirical tool for estimating composition, size, and concentration characteristics of particulate matter from IOPs.

[63] A general prerequisite for pursuing this approach is to establish the desired relationships of the algorithm for the area of interest using a comprehensive suite of measurements that include the IOPs made in tandem with a characterization of concentration, composition, and size distribution of suspended particulate matter. Whereas large amounts of optical data have been collected in recent years, field experiments in which such comprehensive optical and complementary data are acquired concurrently are still scarce. As a consequence, most optical measurements have been amenable to the interpretation in terms of water constituents only at a very general and overly simplistic level that is usually insufficient to explain the observed natural variability. The design and execution of future optical experiments which include complementary detailed analyses of discrete water samples is therefore necessary for continued progress in understanding complex optical environments.

[64] **Acknowledgments.** This study was supported by the National Aeronautics and Space Administration (Earth Observing System Interdisciplinary Science Program, NASA EOS/IDS Grants NNG04GK50G and NNG04GJ38G awarded to D.S. and M.S.) and by the Office of Naval Research Environmental Optics Program (grant N00014-05-1-0246 to D.S.). The analysis of samples for particulate organic carbon was made at Marine Science Institute Analytical Laboratory, University of California Santa Barbara. The fluorometric determinations of chlorophyll *a* concentration was made at the Center for Hydro-Optics and Remote Sensing, San Diego State University. We thank two anonymous reviewers for valuable comments on the manuscript.

References

Aas, E. (1996), Refractive index of phytoplankton derived from its metabolite composition, *J. Plankton Res.*, *18*, 2223–2249.

Anderson, L. A. (1995), On the hydrogen and oxygen content of marine phytoplankton, *Deep Sea Res., Part I*, *42*, 1675–1680.

Babin, M., A. Morel, V. Fournier-Sicre, F. Fell, and D. Stramski (2003a), Light scattering properties of marine particles in coastal and open ocean waters as related to the particle mass concentration, *Limnol. Oceanogr.*, *48*, 843–859.

Babin, M., D. Stramski, G. M. Ferrari, H. Claustre, A. Bricaud, G. Obolensky, and N. Hoepffner (2003b), Variations in the light absorption coefficients of phytoplankton, nonalgal particles, and dissolved organic matter in coastal waters around Europe, *J. Geophys. Res.*, *108*(C7), 3211, doi:10.1029/2001JC000882.

Barillé-Boyer, A.-L., L. Barillé, H. Massé, D. Razet, and M. Héral (2003), Correction for particulate organic matter as estimated by loss on ignition in estuarine ecosystems, *Estuarine Coastal Shelf Sci.*, *58*, 147–153.

Bohren, C. F., and D. R. Huffman (1983), *Absorption and Scattering of Light by Small Particles*, 530 pp., Wiley, New York.

Bowers, D. G., and C. E. Binding (2006), The optical properties of mineral suspended particles: A review and synthesis, *Estuarine Coastal Shelf Sci.*, *67*, 219–230.

Bowers, D. G., G. E. L. Harker, and B. Stephan (1996), Absorption spectra of inorganic particles in the Irish Sea and their relevance to remote sensing of chlorophyll, *Int. J. Remote Sens.*, *17*, 2449–2460.

Carder, K. L., and D. K. Costello (1994), Optical effects of large particles, in *Ocean Optics*, edited by R. W. Spinrad, K. L. Carder, and M. J. Perry, pp. 243–257, Oxford Univ. Press, New York.

Chang, G. C., T. D. Dickey, O. M. Schofield, A. D. Wiedemann, E. Boss, W. S. Pegau, M. A. Moline, and S. M. Glenn (2002), Nearshore physical processes and bio-optical properties in the New York Bight, *J. Geophys. Res.*, *107*(C9), 3133, doi:10.1029/2001JC001018.

Coble, P., C. Hu, R. W. Gould Jr., G. Chang, and M. Wood (2004), Colored dissolved organic matter in the coastal ocean: An optical tool for coastal zone environmental assessment and management, *Oceanography*, *17*(2), 50–59.

Dickey, T. D. (2004), Studies of coastal ocean dynamics and processes using emerging optical technologies, *Oceanography*, *17*(2), 9–13.

Dickey, T. D., and G. Chang (2001), Recent advances and future visions: Temporal variability of optical and bio-optical properties of the ocean, *Oceanography*, *14*(3), 15–29.

DuRand, M. D., R. E. Green, H. M. Sosik, and R. J. Olson (2002), Diel variations in optical properties of Micromonas pusilas (Prasinophyceae), *J. Phycol.*, *38*, 1132–1142.

Ferrari, G. M., and S. Tassan (1999), A method using chemical oxidation to remove light absorption by phytoplankton pigments, *J. Phycol.*, *35*, 1090–1098.

Gallegos, C. L., T. E. Jordan, A. H. Hines, and D. E. Weller (2005), Temporal variability of optical properties in a shallow, eutrophic estuary: Seasonal and interannual variability, *Estuarine Coastal Shelf Sci.*, *64*, 156–170.

Gardner, W. D., A. V. Mishonov, and M. J. Richardson (2006), Global POC concentrations from in-situ and satellite data, *Deep Sea Res., Part II*, *53*, 718–740.

Green, R. E., H. M. Sosik, and R. J. Olson (2003), Contributions of phytoplankton and other particles to inherent optical properties in New England continental shelf waters, *Limnol. Oceanogr.*, *48*, 2377–2391.

Jackson, G. A., R. Maffione, D. K. Costello, A. L. Alldredge, B. E. Logan, and H. G. Dam (1997), Particle size spectra between 1 μm and 1 cm at Monterey Bay determined using multiple instruments, *Deep Sea Res., Part I*, *44*, 1739–1767.

Jonasz, M., and G. R. Fournier (2007), *Light Scattering by Particles in Water: Theoretical and Experimental Foundations*, 704 pp., Academic, Amsterdam.

Kerr, P. F. (1977), *Optical Mineralogy*, 492 pp., McGraw-Hill, New York.

Loisel, H., and A. Morel (1998), Light scattering and chlorophyll concentration in case 1 waters: A reexamination, *Limnol. Oceanogr.*, *43*, 847–858.

McKee, D., and A. Cunningham (2006), Identification and characterization of two optical water types in the Irish Sea from in situ inherent optical properties and seawater constituents, *Estuarine Coastal Shelf Sci.*, *68*, 305–316.

Menden-Deuer, S., and E. J. Lessard (2000), Carbon to volume relationships for dinoflagellates, diatoms, and other protist plankton, *Limnol. Oceanogr.*, *45*, 569–579.

Mitchell, B. G. (1990), Algorithm for determining the absorption coefficient of aquatic particulates using the quantitative filter technique (QFT), in *Proc. SPIE Int. Soc. Opt. Eng.*, *1302*, 137–148.

Mitchell, B. G., M. Kahru, J. Wieland, and M. Stramska (2003), Determination of spectral absorption coefficients of particles, dissolved material and phytoplankton for discrete water samples, in *Ocean Optics Protocols for Satellite Ocean Color Sensor Validation, Revision 4, Volume IV—Inherent Optical Properties: Instruments, Characterizations, Field Measurements and Data Analysis Protocols*, edited by J. L. Mueller, G. S. Fargion, and C. R. McClain, *NASA/TM-2003-211621/Rev4-Vol. IV*, pp. 39–64, Natl. Aeronaut. Space Admin., NASA Goddard Space Flight Cent., Greenbelt, Maryland.

Morel, A., and A. Bricaud (1981), Theoretical results concerning light absorption in a discrete medium, and application to specific absorption of phytoplankton, *Deep Sea Res., Part A*, *28*, 1375–1393.

Montagnes, D. J., J. A. Berges, P. J. Harrison, and F. J. R. Taylor (1994), Estimation of carbon, nitrogen, protein, and chlorophyll *a* from volume in marine phytoplankton, *Limnol. Oceanogr.*, *39*, 1044–1060.

Oubelkheir, K., L. A. Clementson, I. T. Webster, P. W. Ford, A. G. Dekker, L. C. Radke, and P. Daniel (2006), Using inherent optical properties to investigate biogeochemical dynamics in a tropical macrotidal coastal system, *J. Geophys. Res.*, *111*, C07021, doi:10.1029/2005JC003113.

Pearlman, S. R., H. S. Costa, R. A. Jung, J. J. McKeown, and H. E. Pearson (1995), Solids, in *Standard Methods for the Examination of Water and Wastewater*, edited by A. D. Eaton, L. S. Clesceri, and A. E. Greenberg, section 2540, pp. 2-53–2-64, Am. Public Health Assoc., Washington, D. C.

Peng, F., and S. W. Effler (2007), Suspended minerogenic particles in a reservoir: Light-scattering features from individual particle analysis, *Limnol. Oceanogr.*, *52*, 204–216.

Peng, F., S. W. Effler, D. O'Donnell, M. Gail Perkins, and A. Weidemann (2007), Role of minerogenic particles in light scattering in lakes and a river in central New York, *Appl. Opt.*, *46*, 6577–6594.

Philpot, W., C. O. Davis, W. P. Bissett, C. D. Mobley, D. D. R. Kohler, Z. Lee, J. Bowles, R. G. Steward, Y. Agrawal, J. Trowbridge, R. W. Gould Jr., and R. A. Arnone (2004), Bottom characterization from hyperspectral image data, *Oceanography*, *17*(2), 76–85.

Redfield, A. C., B. H. Ketchum, and F. A. Richards (1963), The influence of organisms on the composition of seawater, in *The Sea*, vol. 2, *The Composition of Sea Water: Comparative and Descriptive Oceanography*, edited by M. N. Hill, pp. 26–77, Wiley-Interscience, New York.

Schofield, O., J. Kerfoot, K. Mahoney, M. Moline, M. Oliver, S. Lohrenz, and G. Kirkpatrick (2006), Vertical migration of the toxic dinoflagellate *Karenia brevis* and the impact on ocean optical properties, *J. Geophys. Res.*, *111*, C06009, doi:10.1029/2005JC003115.

Snyder, W. A., R. A. Arnone, C. O. Davis, W. Goode, R. W. Gould, S. Ladner, G. Lamela, W. J. Rhea, R. Stavn, M. Sydor, and A. Weidemann (2008), Optical scattering and backscattering by organic and inorganic particulates in U.S. coastal waters, *Appl. Opt.*, *47*, 666–677.

Stavn, R. H., and S. J. Richter (2008), Biogeo-optics: Particle optical properties and the partitioning of the spectral scattering coefficient of ocean waters, *Appl. Opt.*, *47*, 2660–2679.

Stavn, R. H., H. J. Rick, and A. V. Falster (2009), Correcting the errors from variable sea salt and water of hydration in loss on ignition analysis: Implications for studies of estuarine and coastal waters, *Estuarine Coastal Shelf Sci.*, *81*, 575–582.

Stramska, M., D. Stramski, S. Kaczmarek, D. B. Allison, and J. Schwarz (2006), Seasonal and regional differentiation of bio-optical properties within the north polar Atlantic, *J. Geophys. Res.*, *111*, C08003, doi:10.1029/2005JC003293.

Stramska, M., D. Stramski, M. Cichocka, A. Cieplak, and S. B. Woźniak (2008), Effects of atmospheric particles from Southern California on the optical properties of seawater, *J. Geophys. Res.*, *113*, C08037, doi:10.1029/2007JC004407.

Stramski, D. (1999), Refractive index of planktonic cells as a measure of cellular carbon and chlorophyll a content, *Deep Sea Res., Part I*, *46*, 335–351.

Stramski, D., and D. A. Kiefer (1991), Light-scattering by microorganisms in the open ocean, *Prog. Oceanogr.*, *28*, 343–383.

Stramski, D., R. A. Reynolds, M. Kahru, and B. G. Mitchell (1999), Estimation of particulate organic carbon in the ocean from satellite remote sensing, *Science*, *285*, 239–242.

Stramski, D., A. Bricaud, and A. Morel (2001), Modeling the inherent optical properties of the ocean based on the detailed composition of the planktonic community, *Appl. Opt.*, *40*, 2929–2945.

Stramski, D., E. Boss, D. Bogucki, and K. J. Voss (2004a), The role of seawater constituents in light backscattering in the ocean, *Prog. Oceanogr.*, *61*, 27–56.

Stramski, D., S. B. Woźniak, and P. J. Flatau (2004b), Optical properties of Asian mineral dust suspended in seawater, *Limnol. Oceanogr.*, *49*, 749–755.

Stramski, D., M. Babin, and S. B. Woźniak (2007), Variations in the optical properties of terrigenous mineral-rich particulate matter suspended in seawater, *Limnol. Oceanogr.*, *52*, 2418–2433.

Stramski, D., R. A. Reynolds, M. Babin, S. Kaczmarek, M. R. Lewis, R. Röttgers, A. Sciandra, M. Stramska, M. S. Twardowski, B. A. Franz, and H. Claustre (2008), Relationships between the surface concentration of particulate organic carbon and optical properties in the eastern south Pacific and eastern Atlantic Oceans, *Biogeosciences*, *5*, 171–201.

Tassan, S., and G. M. Ferrari (1995), An alternative approach to absorption measurements of aquatic particles retained on filters, *Limnol. Oceanogr.*, *40*, 1358–1368.

Tassan, S., and G. M. Ferrari (2002), A sensitivity analysis of the 'Transmittance-Reflectance' method for measuring light absorption by aquatic particles, *J. Plankton Res.*, *24*, 757–774.

Trees, C. C. (1978), Analytical analysis of the effect of dissolved solids on suspended solids determination, *J. Water Pollut. Control Fed.*, *50*, 2370–2373.

Trees, C. C., R. R. Bidigare, D. M. Karl, L. Van Heukelem, and J. Dore (2002), Fluorometric chlorophyll a: Sampling, laboratory methods, and data analysis protocols, in *Ocean Optics Protocols for Satellite Ocean Color Sensor Validation*, edited by J. L. Mueller and G. S. Fargion, *NASA/TM-2002-210004/Rev3-Vol2*, pp. 269–283, Natl. Aeronaut. Space Admin., NASA Goddard Space Flight Cent., Greenbelt, Maryland.

Vantrepotte, V., C. Brunet, X. Mériaux, E. Lécuyer, V. Vellucci, and R. Santer (2007), Bio-optical properties of coastal waters in the eastern English Channel, *Estuarine Coastal Shelf Sci.*, *72*, 201–212.

Weisberg, R. H., R. He, G. Kirkpatrick, F. Muller-Karger, and J. J. Walsh (2004), Coastal ocean circulation influences on remotely sensed optical properties: A West Florida Shelf case study, *Oceanography*, *17*(2), 68–75.

Woźniak, S. B., and D. Stramski (2004), Modeling the optical properties of mineral particles suspended in seawater and their influence on ocean reflectance and chlorophyll estimation from remote sensing algorithms, *Appl. Opt.*, *43*, 3489–3503.

M. Cichocka, A. M. Cieplak, E. Y. Miksic, R. A. Reynolds, D. Stramski, and V. M. Wright, Marine Physical Laboratory, Scripps Institution of Oceanography, University of California, San Diego, 9500 Gilman Dr., Mail Code 0238, La Jolla, CA 92093-0238, USA.

M. Stramska, Center for Hydro-Optics and Remote Sensing, San Diego State University, 6505 Alvarado Rd., San Diego, CA 92120, USA.

S. B. Woźniak, Institute of Oceanology, Polish Academy of Sciences, Powstańców Warszawy 55, 81-712 Sopot, Poland. (woznjr@iopan.gda.pl)